NEW PROBLEMS

Charles H. Holbrow, *Editor*
Colgate University, Hamilton, New York 13346

The "New Problems" department presents interesting, novel problems for use in undergraduate physics courses beyond the introductory level. We will publish worked problems that convey the excitement and interest of current developments in physics and that are useful for teaching courses such as Classical Mechanics, Electricity and Magnetism, Statistical Mechanics and Thermodynamics, Modern Physics, or Quantum Mechanics. We challenge physicists everywhere to create problems that show how their various branches of physics use the central, unifying ideas of physics to advance physical understanding. We want these problems to become an important source of ideas and information for students of physics. This project is supported by the Physics Division of the National Science Foundation. Submit materials to Charles H. Holbrow, *Editor*.

Doppler-free saturated absorption: Laser spectroscopy

Daryl W. Preston
Department of Physics, California State University, Hayward, California 94542

(Received 6 July 1995; accepted 22 July 1996)

I. SCOPE

These problems illustrate laser-saturated absorption spectroscopy. They show how this technique circumvents Doppler broadening in measurements of optical spectra and so can improve resolution by several orders of magnitude. Solving these problems requires an understanding of the Boltzmann velocity distribution, the Doppler effect, and basic features of induced absorption of laser light by alkali atoms. The problems are suitable for a course in modern physics and provide background for advanced laboratory experiments in both high-resolution spectroscopy and cooling and trapping of atoms.[1–3]

II. LASER ABSORPTION SPECTROSCOPY

In laser-saturated absorption spectroscopy three beams of light derived from the same laser pass through a cell containing a low-density vapor of atoms. The frequency of the laser light is varied, and resonances are observed by detecting increases in absorption when the frequency matches a transition frequency of atoms in the vapor.

A. Rubidium

Rubidium is a convenient atom to study with absorption spectroscopy. Because it has a single electron outside of closed shells, it has a relatively simple hydrogenlike structure of energy levels. The ground and first excited states of the single electron are, respectively, $5^2S_{1/2}$ and $5^2P_{1/2,3/2}$, and, although the $I=3/2$ nuclear spin of ^{87}Rb produces the hyperfine splittings shown in Fig. 1, the transitions shown there all have wavelengths around 780 nm and are easily induced with a compact, inexpensive diode laser. Rubidium's high vapor pressure permits it to be used in a vapor cell at room temperature. The feasibility of doing without a complicated oven and also using a diode laser means that the apparatus for laser absorption spectroscopy of rubidium can be quite simple.

B. A laser saturated absorption spectrometer

Figure 2 is a diagram of a laser spectrometer based on a tunable diode laser like that described in Ref. 2. The laser frequency can be swept through the atomic absorption lines by varying the voltage across a piezoelectric transducer (PZT) to change the length of the laser's cavity.

The 780-nm wavelength light from the laser is divided into three beams. The most intense beam is called the "pump" beam. The other two beams, which are of considerably lower intensity than the pump beam, are sent through the vapor cell in the direction opposite that of the pump beam. These are called the "probe" beams and each is detected by a photodiode. The probe beam that is arranged to overlap the counterpropagating pump beam inside the cell is called the "overlap" beam; the other probe beam, which does not overlap with the pump beam, is called the "reference beam."

For reasons made clearer below, the signals produced by the two probe beams at the photodiodes are adjusted to be equal and then subtracted from each other. It is the difference between the two signals that is usually recorded.

III. DOPPLER BROADENED ABSORPTION SPECTRA

In conventional laser spectroscopy the closely spaced spectral lines arising from atomic fine structure or hyperfine structure are often not resolved because of Doppler broadening. When the overlap probe beam is blocked so that it does not reach the photodiode, the absorption signal then comes only from the reference probe beam and displays Doppler broadened absorption lines. Figure 3(a) shows such a spectrum. Here, the stronger line is due to ^{85}Rb (72% natural abundance) and the weaker line is due to ^{87}Rb (28% natural abundance). The ^{87}Rb line arises from the three $5^2S_{1/2}(F=2)\rightarrow 5^2P_{3/2}(F'=1,2,3)$ transitions (see Fig. 1), but these appear together as one line in the data of Fig. 3(a) because of Doppler broadening.

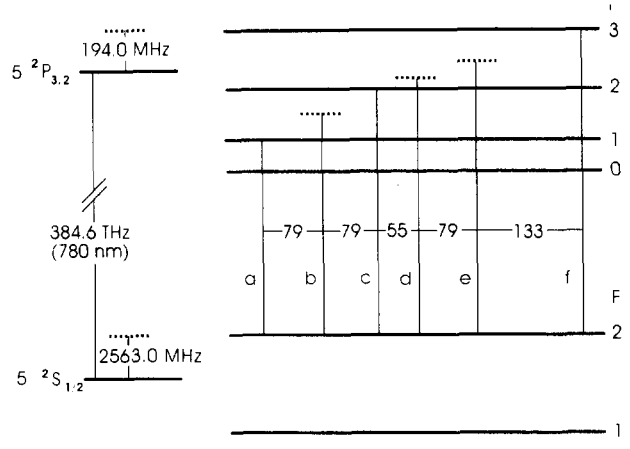

Fig. 1. Hyperfine levels and $F=2\rightarrow F'=1,2,3$ transitions for ^{87}Rb. The numbers 79, 79, etc., are accepted values of line separations in MHz. The horizontal dashed lines correspond to crossover frequencies as explained in the text. The diagram of the overall transition shown at the left is not linearly scaled.

This well-known effect arises because the atoms have a thermal (Maxwellian) distribution of velocities. If a vapor of atoms is irradiated by laser light, thermal motion will cause most of the atoms to receive the incident light at frequencies Doppler shifted away from the laser frequency. Thus, for example, if the laser is tuned exactly to the atoms' resonant frequency ν_1, only those atoms that have no component of velocity along the line of the incident light will be resonant with it. Those atoms which have a component of velocity v_z along the axis of the laser beam will become resonant only when the laser frequency is tuned to

$$\nu=\nu_1\left(1+\frac{v_z}{c}\right), \tag{1}$$

where c is the speed of light. Equation (1) is just the equation for the Doppler shift of light when $v_z \ll c$ as is the case here. Put another way, when the laser light is tuned to frequency ν, the light will be resonant with just those atoms that have velocity along the laser beam of

$$v_z=\left(\frac{\nu-\nu_1}{\nu_1}\right)c. \tag{2}$$

When $v_z>0$, the atoms are moving in the direction of the laser beam; when $v_z<0$, they are moving opposite to the light.

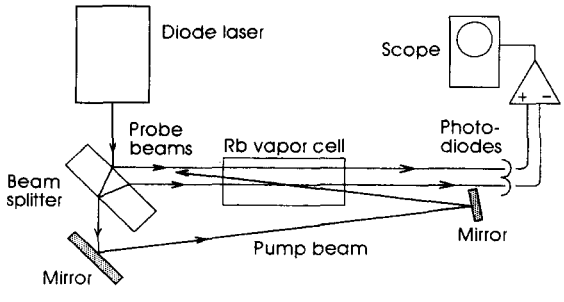

Fig. 2. A laser-diode, saturated absorption spectrometer.

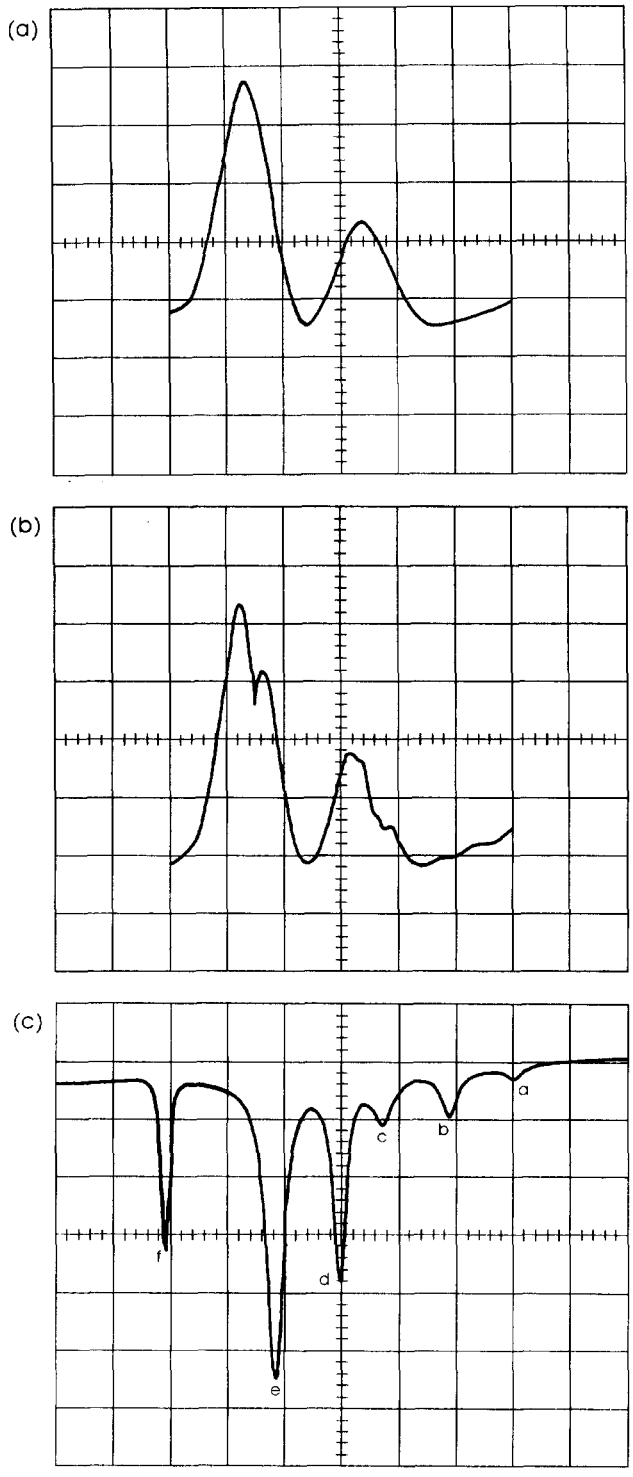

Fig. 3. Experimentally observed spectral lines of ^{87}Rb, where frequency is increasing to the left: (a) Doppler broadened spectral lines; (b) Doppler broadened lines with dips; (c) saturated absorption lines, where the labels on the lines correspond to the labels in Fig. 1. In (a) and (b) one horizontal division=534 MHz; in (c) one horizontal division=69 MHz.

This means that as the frequency ν of the laser is varied, the light interacts with different parts of the thermal distribution of the velocities of the atoms. A graph of absorption as a function of laser frequency ν will have the shape of the

v_z velocity distribution of the atoms, which for atoms in thermal equilibrium is just the Maxwellian distribution of the z component of the velocities:

$$e^{-Mv_z^2/2k_BT}, \tag{3}$$

where k_B is the Boltzmann constant (1.38×10^{-23} J/K), M is the mass of an atom, and T is the temperature of the vapor.

IV. DOPPLER PROBLEMS

A. Doppler broadened absorption line shape

By substituting Eq. (2) into Eq. (3) show that the relative number of atoms in a vapor that are resonant with light in a range of frequencies around ν_1 is given by the Gaussian function

$$e^{-Mc^2(\nu-\nu_1)^2/2k_BT\nu_1^2}. \tag{4}$$

B. Calculated Doppler linewidth

Show that this distribution has a full width at half maximum of

$$\Delta\nu_{1/2}=\sqrt{8k_B\ln 2}\,\frac{\nu_1}{c}\sqrt{\frac{T}{M}}=2.92\times10^{-20}\nu_1\sqrt{\frac{T}{M}}\ \text{Hz}, \tag{5}$$

where ν_1 is in hertz, M is in kilograms, and T is in Kelvins. This quantity $\Delta\nu_{1/2}$ is the linewidth due to Doppler broadening.

C. Observed Doppler linewidth

In Fig. 3(a) the calibration of the horizontal axis is 534 MHz/div (where "div" means major division on the oscilloscope screen). Use this fact to determine the ^{87}Rb absorption linewidth from the data. Compare this result with what you would expect from Eq. (5).

D. Resolving power

From your values of the Doppler broadened linewidths, estimate the resolving power of this kind of laser absorption spectroscopy.

V. DOPPLER ANSWERS

A. Doppler broadened line shape

To find the linewidth, note that you want the value of $\Delta\nu_{1/2}\equiv2(\nu-\nu_1)$ for which Eq. (4) equals 1/2; i.e.,

$$\tfrac{1}{2}=e^{-Mc^2\Delta\nu_{1/2}^2/4k_BT\nu_1^2}.$$

Take the internal log of both sides, and solve for $\Delta\nu_{1/2}$.

B. Experimentally observed linewidth

Direct measurement from Fig. 3(a) shows the full width at half maximum of the curve is about 1.05 divisions on the oscilloscope screen. From the calibration given above, the width must be $534\times1.05=561$ MHz.

To obtain the Doppler linewidth from Eq. (5) substitute in the mass of the absorbing atom, $M=87\times1.67\times10^{-27}$ kg, the temperature, $T\approx300$ K, and the resonance frequency of an atom in the rest frame of the laser, $\nu_1=(3\times10^8)/(780\times10^{-9})=3.85\times10^{14}$ Hz. From Eq. (5) the calculated linewidth for ^{87}Rb at room temperature is 513 MHz.

C. Resolving power

The frequency separation of the well-resolved Doppler broadened lines shown in Fig. 3(a) is approximately 534 MHz/div$\times$2 div$=$1.1 GHz. If the spacing were about 1 div or 534 MHz, then the lines would be barely resolved. Hence, the resolving power is $\nu_1/\Delta\nu=7\times10^5$.

VI. LASER SATURATED ABSORPTION SPECTROSCOPY

In the early 1970s Schawlow and Hänsch[4] developed a practical way to use nonlinear interactions of laser light with atoms to produce spectra without Doppler broadening. Their technique, known as laser-saturated absorption spectroscopy, grew out of fundamental work on nonlinear optics done by them and other physicists, e.g., Bloembergen, Lamb, and Javan.[5]

In this technique, two counterpropagating, overlapping laser beams of exactly the same frequency interact with atoms in a vapor. When the laser frequency is different from the resonant frequency of the atoms, ν_1, one beam interacts with a set of atoms with some velocity v_z and the other beam interacts with an entirely different set of atoms, those with velocity $-v_z$. However, when the frequency is tuned to ν_1, the two beams interact with the same group of atoms, those with velocity component parallel to the beams ≈0. Under these circumstances the stronger beam, the pump beam, reduces the absorption experienced by the weaker overlap probe beam but only over a very narrow range of frequencies that under proper conditions can approach the natural width determined by the lifetime of the atomic transition.

A. Laser saturated absorption spectrum

To see how the narrow absorption dip arises, consider what happens when the reference probe beam is blocked and only the overlap probe beam is allowed to strike its photodiode. Figure 3(b) shows that there appear "dips" in the spectral lines. To understand these it helps to look at Fig. 4, which shows the number of atoms in the ground state, $N_{gs}(v_z)$ as a function of atomic velocity v_z (where positive v_z is parallel to the probe beams). In Fig. 4(a) the laser frequency ν is less than ν_1, the frequency of a transition from a ground-state F level to an excited F' level. The notch to the left corresponds to atoms moving in the negative direction with exactly the correct velocity $-v_{z1}$ to see the overlap probe beam blueshifted to ν_1; as a result, the number of atoms in the ground state is reduced as shown in Fig. 4(a). A different group of atoms with the positive velocity v_{z1} will see the pump beam also blueshifted to ν_1, and the number of ground-state atoms with this velocity will be reduced as shown by the notch on the right. For $\nu\neq\nu_1$ the two beams interact with these two different groups of atoms, and as ν is increased, the notch due to the pump beam moves left and that due to the probe beam moves right.

When $\nu=\nu_1$ as in Fig. 4(b), the two beams interact with the same group of atoms. Then the pump beam depletes the number of atoms in the ground-state F level, and the probe beam passes through the vapor cell with reduced absorption, so that "dips" appear in the Doppler broadened absorption line, as shown in Fig. 3(b).

The two photodiodes shown in Fig. 2 are wired so that their signals subtract. If neither probe beam is blocked, the signals shown in Fig. 3(a) and Fig. 3(b) are subtracted, and the resulting signal is like that in Fig. 3(c).

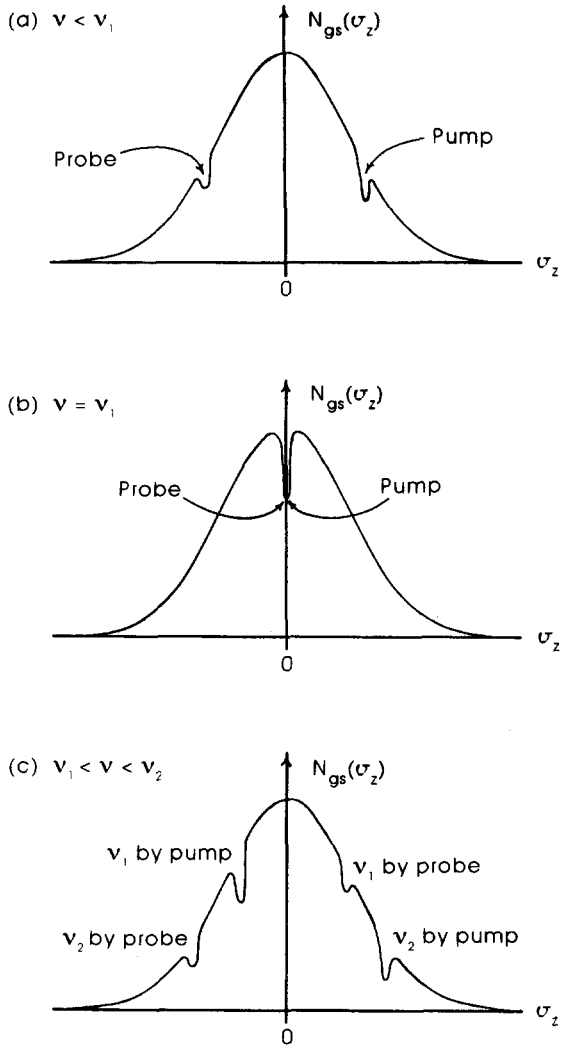

Fig. 4. Absorption of pump and probe beams by ground-state atoms depends on the Doppler shift of the laser frequency ν to the transition frequency ν_1 by the atoms' thermal velocity: (a) $\nu<\nu_1$; (b) $\nu=\nu_1$ and (c) the crossover situation when $\nu_1<\nu<\nu_2$ and the two transitions ν_1 and ν_2 are within a Doppler width of each other.

The three dips labeled a, c, and f in Fig. 3(c) correspond to the atomic transitions labeled a, c, and f in Fig. 1. The three dips labeled b, d, and e in Fig. 3 are known as "crossover" dips and are peculiar to saturated absorption spectroscopy.

B. Crossover transitions

A crossover dip can occur when two transitions share a common ground state and differ in frequency by less than the Doppler linewidth. In this situation there are laser frequencies at which the pump beam interacts with two different groups of atoms at the same time. An example is shown in Fig. 4(c), where $\nu_1<\nu<\nu_2$ so that the atoms with velocity $-v_{z1}$ see ν redshifted to ν_1, while at the same time those with velocity $+v_{z2}$ see ν blueshifted to ν_2. The probe beam interacts in a similar way with atoms at $+v_{z1}$ and $-v_{z2}$. As the laser frequency is increased, the notches corresponding to the pump beam move left, and those of the probe beam move right. Clearly, there will be some laser frequency ν_c such that the same group of atoms will be resonant at ν_1 with the pump and at ν_2 with the probe (and another group at ν_1 with the probe and ν_2 with the pump). In both cases the pump beam reduces the population in the $F=2$ level, and there is increased transmission of the overlapping probe beam giving rise to the extra dips, b, d, and e in Fig. 3.

VII. SOME SATURATION SPECTROSCOPY PROBLEMS

A. What is the crossover frequency?

Show that the crossover frequency ν_c is

$$\nu_c=\frac{\nu_1+\nu_2}{2}.$$

B. What levels produce the crossovers?

The horizontal dashed lines on the right-hand level diagram in Fig. 1 correspond to crossover frequencies giving rise to the dips labeled b, d, and e in Fig. 3(c). Identify what two atomic transitions are involved in each case and verify that they differ in frequency by less than the Doppler width.

C. Saturation spectroscopy linewidths

What are the widths of lines e and f in Fig. 3(c)? Given that the lifetime of these atomic states is about 28 ns, calculate the natural linewidth predicted by the Heisenberg uncertainty principle and compare it with your measured linewidth.

D. Resolving power

From your values of the widths of the lines in Fig. 3(c) estimate the resolving power exhibited in these saturation laser spectroscopy data.

VIII. ANSWERS TO SATURATION SPECTROSCOPY PROBLEMS

A. What is the crossover frequency?

The crossover occurs when the laser frequency ν_c is such that atoms with velocity $-v_{z1}$ see the pump beam Doppler redshifted to the transition frequency ν_1 and at the same time see the probe beam blueshifted to ν_2. In other words,

$$\nu_1=\nu_c-\frac{v_{z1}}{c}\,\nu_c$$

and

$$\nu_2=\nu_c+\frac{v_{z1}}{c}\,\nu_c.$$

Adding these two equations and solving for ν_c gives

$$\nu_c=\frac{\nu_1+\nu_2}{2}$$

exactly halfway between the two transition frequencies.

B. Crossover frequencies in the Rb hyperfine spectrum

The crossover peaks marked b, d, and e arise, respectively, from the pairs of transitions $F=2\rightarrow F'=1$ and $F=2\rightarrow F'=2$; $F=2\rightarrow F'=1$ and $F=2\rightarrow F'=3$; and $F=2\rightarrow F'=2$ and $F=2\rightarrow F'=3$.

These three crossover frequencies are shown in the diagram of Fig. 1 by the vertical lines labeled b, d, and e connecting dashed horizontal lines to the $F=2$ groundstate level. The frequency separations between transitions are labeled horizontally across the middle of the diagram, 79, 79, etc. They show that all three of the observed hyperfine transitions fall within about 400 MHz of each other, well within the observed Doppler width of 561 MHz.

C. Linewidths

In Fig. 3(c) the horizontal axis was calibrated to be 69 MHz/div. Consequently, the linewidths of the saturated absorption dips e and f shown there are respectively approximately $69\times0.40=28$ MHz and $69\times0.18=13$ MHz.

The natural linewidth predicted by the Heisenberg uncertainty principle for a state with lifetime $\tau=28$ ns is $\Delta\nu=1/(2\pi\tau)=6$ MHz, which is 1/2 to 1/5 of what is measured.

Spectral linewidths depend on the rate at which the atoms are undergoing collisions, on the particular gas species present in the cell, and on the rate at which the laser light stimulates the observed transitions. They also depend on the spread of frequencies in the laser light itself, but, since this is no more than a few MHz for the laser used here, the discrepancy between the observed value of $\Delta\nu$ and the value predicted by the uncertainty principle is probably due to a combination of the other effects.

D. Resolving power

The frequency separation of spectral lines labeled e and f is 69 MHz/div$\times$1.9 div$=$131 MHz. If the separation was about 0.3 div or 21 MHz, the peaks would be barely resolved. Hence, the resolving power is about 18×10^6, a more than 20-fold improvement over the resolving power of ordinary linear spectroscopy.

ACKNOWLEDGMENT

The author is indebted to Carl Wieman, University of Colorado, for providing Fig. 3(c).

[1]Drayl W. Preston and Carl E. Wieman, "Doppler-free saturated absorption spectroscopy: laser spectroscopy," an unpublished advanced laboratory writeup available from Daryl W. Preston, e-mail: dpreston@csuhayward.edu

[2]K. D. MacAdam, A. Steinbach, and C. Wieman, "A narrow-band tunable diode laser system with grating feedback, and a saturated absorption spectrometer for Cs and Rb," Am. J. Phys. **60**, 1098–1111 (1992).

[3]Carl Wieman, Gwenn Flowers, and Sarah Gilbert, "Inexpensive laser cooling and trapping experiment for undergraduate laboratories," Am. J. Phys. **63**, 317–330 (1995).

[4]Arthur L. Schawlow, "Spectroscopy in a new light," Rev. Mod. Phys. **54**, 697–707 (1982) (1981 Nobel lecture).

[5]Nicolaas Bloembergen, "Nonlinear optics and spectroscopy," Rev. Mod. Phys. **54**, 685–695 (1982) (1981 Nobel lecture).

ASSEMBLY LANGUAGE PROGRAMMING

What you can't see in the picture is that this machine was programmed entirely in assembly language. Over 4000 statements on punch cards were eventually written for the analysis codes. Also, due to the limited hardware of the system (16K memory, no disk drive), I could not use the available operating systems provided by the manufacturer, which would have been too large and slow for the purposes of this application anyway. Hence the task of programming the computer also involved writing my own custom drivers for the peripherals, servicing the interrupts, and the like. I do recall a certain sense of pride that every bit set and every action carried out by that machine was explicitly controlled by code that I had written. I also recall saying when it was done that while it had been quite a valuable and interesting experience to understand and program a computer so extensively at such a fundamental level, once in a lifetime for this type of experience was enough!

Russell A. Hulse (Nobel Lecture, December 8, 1993) "The Discovery of the Binary Pulsar," Reviews of Modern Physics, **66** (3), 699–710 (1994).

DOPPLER-FREE SATURATED ABSORPTION SPECTROSCOPY:

LASER SPECTROSCOPY

Daryl W. Preston
California State University, Hayward
Carl E. Wieman
University of Colorado, Boulder

Adapted for Reed College by Morgan Mitchell

Historical Note

One half of the 1981 Nobel prize in Physics was awarded jointly to:
Nicolaas Bloembergen, the United States, Harvard University, Cambridge Massachusetts, and
Arthur L. Schawlow, the United States, Stanford University, Stanford, California
For their contribution to the development of laser spectroscopy
and the other half to
Kai M. Siegbahn, Sweden, Uppsala University, Uppsala, Sweden
For his contribution to the development of high resolution electron spectroscopy.

During the 70's Professor Schawlow's research group developed and applied the technique of Doppler-Free Saturation Absorption Spectroscopy, and, at that time, Professor Wieman was a graduate student in the group.

Apparatus

Tunable 780-nm diode laser system (see reference 1)
Rubidium vapor cell
Photodiode detector circuit
Triangle waveform generator
3/8"-thick transparent plastic or glass (beam splitter)
4 flat mirrors
4 mirror mounts
9 posts (for mounting vapor cell, photodiode detectors, mirrors, and beam splitter)
Oscilloscope (Optional: storage scope with a plotter)
Oscilloscope camera
IR detection card
Hand held IR viewer or a CCD surveillance camera

Objectives

To appreciate the distinction between linear and nonlinear optics.
To understand term states, fine structure, and hyperfine structure of rubidium.
To record and analyze the Doppler-broadened 780-nm rubidium spectral

line (linear optics).
To record and analyze the Doppler-free saturated absorption lines of rubidium (nonlinear optics).
To construct an interferometer for calibration purposes.

Key Concepts

Linear optics	Electric dipole selection rules
Nonlinear optics	Doppler broadening
Term states	Absorption spectroscopy
Fine structure	Saturated absorption spectroscopy
Hyperfine structure	Crossover resonances
Interferometer	

References

1. K. B. MacAdam, A. Steinbach, and C. Wieman, Am. J. Phys. **60**, 1098-1111, 1992. The construction of the diode laser system and the Doppler-free saturated absorption experiment are discussed in detail in this paper. Parts, suppliers, and cost are listed.
2. M. D. Levenson, Introduction to Nonlinear Laser Spectroscopy, Academic Press, 1982.
3. Carl E. Wieman and Leo Hollberg, Rev. Sci. Instrum. **62**(1), January 1991, pp. 1-20. Diode lasers in atomic physics are reviewed. The list of references is extensive.
4. Daryl W. Preston, Am. J. Phys. **64**, 1432-1436, 1996. This paper is a publication in the "New Problems" section of AJP.
5. A. Corney, Atomic and Laser Spectroscopy, Oxford Press, 1977. Hyperfine interactions are discussed in chapter 18.
6. V. S. Letokhov, "Saturation Spectroscopy", Chapter 4 of High Resolution Laser Spectroscopy (Topics in Applied Physics, Vol. 13, ed. K. Shimoda), Springer-Verlag, 1976.
7. T. W. Hansch, Nonlinear high resolution spectroscopy of atoms and molecules, in "Nonlinear Spectroscopy" (Proc. Int. School Phys., Enrico Fermi, Course 64) (N. Bloemberger, ed.). North-Holland Publi. Amsterdam, 1977.
8. W. Demtroder, Laser Spectroscopy (Springer series in Chemical Physics, Vol. 5), Springer, New York, 1982.
9. E. Arimondo, M. Inguscio, and P.Violino, Rev. Mod. Phys., Vol. 49, No. 1, 1977. The experimental determinations of the hyperfine structure in the alkali atoms are reviewed.
10. R. Gupta, Am. J. Phys. **59**(10), 874 (1991). This paper is a Resource Letter that provides a guide to literature on laser spectroscopy.
11. T. W. Hansch, A. L. Schawlow, and G. W. Series, Sci. Am. **240**(18), 94 (March 1979). An excellent semi-quantitative discussion of laser spectroscopy with many good figures.
12. Jeff Dunham, Modern Physics Laboratory Manual. Doppler-free saturated absorption experiment using a dye laser is described. This excellent lab manual is available by writing Jeff Dunham, Physics Department, Middlebury

College, Middlebury, VT 05753

13. John R. Brandenberger, Lasers and Modern Optics in Undergraduate Physics. Doppler-free saturated absorption experiment using a diode laser is described. This excellent lab manual may be obtained by writing to John Brandenberger, Physics Department, Lawrence University, Appleton, Wisconsin 54912.

14. Daryl W. Preston, Tunable Diode Laser with Grating Feedback. Copies of this experiment are available from the author.

15. Daryl W. Preston and Eric R. Dietz, The Art of Experimental Physics, John Wiley & Sons, 1991.

Introduction

Figure 1 compares an older method with a modern method of doing optical spectroscopy. Figure 1a shows the energy levels of atomic deuterium and the allowed transitions for n = 2 and 3, 1b shows the Balmer α emission line of deuterium recorded at 50 K with a spectrograph, where the vertical lines in 1b are the theoretical intensities, and 1c shows an early high resolution laser measurement, where one spectral line is arbitrarily assigned 0 cm^{-1}. The "crossover" resonance line shown in 1c will be discussed later. Even at 50 K the emission lines are Doppler-broadened by the random thermal motion of the emitting atoms, while the laser method using a technique known as Doppler-free, saturated absorption spectroscopy eliminates Doppler-broadening.

What feature of the laser gives rise to high resolution spectroscopy? Well, it is the narrow spectral linewidth, which is about 20 MHz for the diode laser, and the tunability of lasers that have revolutionized optical spectroscopy. Note that when the 780-nm diode laser is operating at its center frequency then most of its power output is in the frequency range of 3.85×10^{14} Hz $\pm$ 10×10^{6} Hz. Reference 1 points out a method of reducing the spectral linewidth to less than 1 MHz.

The topics to be discussed in the Introduction are linear and nonlinear optics, atomic structure of rubidium, absorption spectroscopy and Doppler broadening, and Doppler-free saturated absorption spectroscopy.

Linear and Nonlinear Optics

The linear formulation of Maxwell's equations assumes that the electric susceptibility χ_e and the magnetic susceptibility χ_m are independent of the strengths of the applied fields. In this case the electric polarization **P** and the magnetization **M** are linearly proportional to the fields:

$$P_i = \chi_{e,ij} E_j \quad (C/m^2); \qquad M_i = \chi_{m,ij} H_j \quad (A/m) \qquad (1)$$

where the subscripts denote cartesian coordinates. Note that **P** and **E**, for example, are not necessarily parallel, i.e., the susceptibility is a tensor, which is a property of some crystals.

If the fields are adequately strong then **P** and **M** are not linear functions of **E** and **H.** For example, the electric polarization is described as a power series in the electric field.

$$P_i = \chi^{e,ij}E_j + \chi^{e,ijk}{}^{(2)}E_jE_k + \chi^{e,ijkl}{}^{(3)}E_jE_kE_l + \qquad (2)$$

In this expansion $\chi^{e,ij}$ is the normal or linear susceptibility and $\chi^{e,ijk}$,etc. are called nonlinear susceptibilities, and the nonlinear optical effects in saturated absorption result from the nonlinear terms. The linear susceptibility is generally much larger than the nonlinear susceptibilities. In equation 2 note that the nonlinear terms are quadratic, cubic, etc. in the electric field. In linear spectroscopy the field measured at the detector is a linear function of the field incident on the sample. A simplified diagram of linear spectroscopy is shown in figure 2a, where a single propagating wave is incident on the sample, some photons are absorbed, as shown in the two-level energy diagram, and some fraction of the wave reaches the detector. Nonlinear spectroscopy is illustrated in figure 2b, where there are two counterpropagating waves that interact with the same atoms in the region where they intersect. The beam propagating to the right, the "pump" beam, causes the transition indicated with a dashed line in the energy level diagram, and the beam propagating to the left, the "probe" beam, causes the transition indicated with a solid line. In this case the field reaching the detector is a function of both fields, hence, nonlinear spectroscopy.

Prior to the development of the laser, the interaction between optical frequency fields and matter were weak enough that linear theories were adequate.

Atomic Structure of Rubidium

The ground electron configuration of Rb is: $1s^2$; $2s^2$, $2p^6$; $3s^2$, $3p^6$, $3d^{10}$; $4s^2$, $4p^6$; $5s^1$, and with its single $5s^1$ electron outside of closed shells it has an energy-level structure that resembles hydrogen. For Rb in its first excited state the single electron becomes a $5p^1$ electron. Also natural rubidium has two isotopes, the 28% abundant ^{87}Rb, where the nuclear spin quantum number I = 3/2, and the 72% abundant ^{85}Rb, where I = 5/2.

Term States

A term state is a state specified by the angular momenta quantum numbers s, l, and j (or S, L, and J), and the notation for such a state is $^{2s+1}l_j$ (or $^{2S+1}L_J$). The spectroscopic notation for l values is l = 0(S), 1(P), 2(D), 3(F), 4(G), 5(H),. . .

The total angular momentum **J** is defined by

$$\mathbf{J} = \mathbf{L} + \mathbf{S} \quad \text{(Joule-seconds)} \qquad (3)$$

where their magnitudes are

$$J = \hbar\sqrt{j(j+1)};\ L = \hbar\sqrt{l(l+1)};\ S = \hbar\sqrt{s(s+1)} \qquad (4)$$

and the possible values of the total angular momentum quantum number j are $|l - s|, |l - s| + 1, \ldots, l + s - 1, l + s$; where for a single electron $s = 1/2$.

The $5s^1$ electron gives rise to a $5^2S_{1/2}$ ground term state. The first excited term state corresponds to the single electron becoming a $5p^1$ electron, and there are two term states, the $5^2P_{1/2}$ and the $5^2P_{3/2}$.

Exercise 1

Show for a $5s^1$ electron that the term state is a $5^2S_{1/2}$. For a $5p^1$ electron show that the term states are $5^2P_{1/2}$ and $5^2P_{3/2}$.

Hamiltonian

Assuming an infinitely massive nucleus, the nonrelativistic Hamiltonian for an atom having a single electron is given by

$$H = \frac{p^2}{2m} - \frac{Z_{eff}e^2}{4\pi\varepsilon_0 r} + \zeta(r)\,L\cdot S + \alpha(J\cdot I) + H_{2,hyp} \quad \text{(Joules)}$$

K V H_{so} $H_{1,hyp}$ $H_{2,hyp}$

$$H_{2,hyp} = \frac{\beta}{2I(2I-1)J(2J-1)}\left[3(I\cdot J)^2 + \frac{3}{2}(I\cdot J) - I(I+1)J(J+1)\right]$$

K is the kinetic energy of the single electron; where $\mathbf{p} = -ih\nabla$, classically $\mathbf{p}$ is the mechanical momentum of the electron of mass m.

V is the Coulomb interaction of the single electron with the nucleus and the core electrons (this assumes the nucleus and core electrons form a spherical symmetric potential with charge $Z_{eff}e$, where Z_{eff} is an effective atomic number).

H_{so} is the spin orbit interaction, where $\mathbf{L}$ and $\mathbf{S}$ are the orbital and spin angular momenta of the single electron.

$H_{1,hyp}$ is the magnetic hyperfine interaction, where $\mathbf{J}$ and $\mathbf{I}$ are the total electron and nuclear angular momenta, respectively. This interaction is $-\mu^n \bullet \mathbf{B}_e$, where μ^n, the nuclear magnetic dipole moment, is proportional to $\mathbf{I}$, and $\mathbf{B}_e$, the magnetic field produced at the nucleus by the single electron, is proportional to $\mathbf{J}$. Hence the interaction is expressed as $\alpha \mathbf{I}\bullet\mathbf{J}$. α is called the magnetic hyperfine structure constant, and it has units of energy, that is, the angular momenta $\mathbf{I}$ and $\mathbf{J}$ are dimensionless.

$H_{2,hyp}$ is the electric quadrupole hyperfine interaction, where β is the electric quadrupole interaction constant, and nonbold I and J are angular momenta quantum numbers. The major electric pole of the Rb nucleus is the spherical symmetric electric monopole, which gives rise to the Coulomb interaction; however, it also has an electric quadrupole moment (but not an electric dipole moment). The electrostatic interaction of the

single electron with the nuclear electric quadrupole moment is $-eV_q$, that is, it is the product of the electron's charge and the electrostatic quadrupole potential. Although it is not at all obvious, this interaction can be expressed in terms of **I** and **J**. In both hyperfine interactions **I** and **J** are dimensionless, that is, the constants α and β have units of joules.

We will not use the above Hamiltonian in the time independent Schrodinger equation and solve for the eigenvalues or quantum states of Rb, but rather we present a qualitative discussion of how each interaction effects such states.

K + V

The K + V interactions separate the 5s ground configuration and the 5p excited configuration. This is shown in figure 3a. Qualitatively, if the potential energy is not a strictly Coulomb potential energy then for a given value of n, electrons with higher l have a higher orbital angular momentum (a more positive kinetic energy) and on the average are farther from the nucleus (a less negative Coulomb potential energy), hence higher l value means a higher (more positive) energy. This scenario does not occur in hydrogen because the potential energy is coulombic.

Fine Structure; H_{so}

The spin-orbit interaction and its physical basis are discussed in Experiment 16, reference 15. Fine structure is discussed in Experiment 12, reference 15, where it is pointed out that fine structure, the splitting of spectral lines into several distinct components, is found in all atoms. The interactions that give rise to fine structure does depend on the particular atom. Ignoring relativistic terms in H, it is H_{so} that produces the fine structure splitting of Rb.

Using equation (3) and forming the dot product of $\mathbf{J}\cdot\mathbf{J}$, we solve for $\mathbf{L}\cdot\mathbf{S}$ and obtain

$$\begin{aligned}\mathbf{L}\cdot\mathbf{S} &= (\mathbf{J}^2 - \mathbf{L}^2 - \mathbf{S}^2)/2 \\ &= (h^2/2)[j(j+1) - l(l+1) - s(s+1)] \qquad (6)\end{aligned}$$

where the magnitudes of the vectors were used in the last equality. Using equation (6), H_{so} can be written

$$H_{so} = \zeta(r)(h^2/2)[j(j+1) - l(l+1) - s(s+1)] \qquad (7)$$

Exercise 2

Show that the splitting of the $5^2P_{1/2}$ and the $5^2P_{3/2}$ term states due to H_{so} is $\zeta(r)3h^2/2$.

Figure 3b shows the effect of H_{so} on the quantum states. The separation of the $5^2S_{1/2}$ and the $5^2P_{3/2}$ states, in units of wavelength, is 780.023 nm, and the separation of the $5^2S_{1/2}$ and the $5^2P_{1/2}$ states

is 794.764 nm. It is the transition between the $5^2S_{1/2}$ and the $5^2P_{3/2}$ states that will be studied using the 780-nm laser.

Hyperfine Structure; H_{hyp}

For either hyperfine interaction, the interaction couples the electron angular momentum **J** and the nuclear angular momentum **I** to form the total angular momentum, which we label as **F**, where

$$\mathbf{F} = \mathbf{J} + \mathbf{I} \tag{8}$$

and the possible quantum numbers F are $|J - I|$, $|J - I + 1|$, .. , $J + I - 1$, $J + I$. (In this case the nonbold capital letters are being used for quantum numbers, which, for the hyperfine interaction, is more standard practice than using f, j and i as the quantum numbers.)

Exercise 3.

For ^{87}Rb show: (1) for the $5^2S_{1/2}$ state that F = 1,2; (2) for the $5\ ^2P_{1/2}$ state that F = 1,2; (3) for the $5^2P_{3/2}$ state that F = 0,1,2,3.

The hyperfine structure of both ^{85}Rb and ^{87}Rb will be observed in this experiment; however, it is the hyperfine structure of ^{87}Rb that will be studied. The energy levels in figure 3b are split by the hyperfine interaction into the levels shown in 3c for ^{87}Rb. The levels in 3c are known as hyperfine levels, where the total angular momentum quantum numbers are labeled as F′ and F for the $5^2P_{3/2}$ and the $5^2S_{1/2}$ states, respectively. The selection rules for electric dipole transitions are given by

$$\begin{aligned} \Delta F &= 0 \text{ or } \pm 1 \text{ (but not } 0 \rightarrow 0) \\ \Delta J &= 0 \text{ or } \pm 1 \\ \Delta S &= 0 \end{aligned} \tag{9}$$

Exercise 4.

Assuming all of the spectral lines are resolved for transitions from the $5^2P_{3/2}$ excited state to the $5^2S_{1/2}$ ground state, how many spectral lines do you expect to observe for ^{87}Rb?

In addition to the ordinary transitions there are "crossover" resonances (which will be discussed later) peculiar to saturated absorption spectroscopy. A crossover resonance is indicated in figure 1c. The crossover transitions are often more intense than the normal transitions. In figure 4 six crossover transitions, b,d,e,h,j and k, and six ordinary transitions, a,c,f,g,i and l, are shown, where for the ordinary transitions $\Delta F = 0, \pm 1$. The frequency of the emitted radiation increases from a to l.

What are the expected frequencies of the ordinary transitions a,c,f,g,i and l? To answer this question we first determine the energies of the hyperfine levels. Using equation 8 and forming the dot product of $\mathbf{F}\cdot\mathbf{F}$, we solve for $\mathbf{J}\cdot\mathbf{I}$ and obtain

$$\mathbf{J}\cdot\mathbf{I} = (\mathbf{F}^2 - \mathbf{J}^2 - \mathbf{I}^2)/2$$
$$= [F(F + 1) - J(J + 1) - I(I + 1)]/2$$
$$\equiv C/2 \qquad (10)$$

where dimensionless magnitudes were used in the second equality and the last equality defines C. Replacing $\mathbf{J}\cdot\mathbf{I}$ in the hyperfine interactions of equation 5 with equation 10, the magnitude of the interactions or the energy $E_{J,F}$ is given by

$$E_{J,F} = E_J + E_{hyp}$$

$$= E_J + \alpha\frac{C}{2} + \beta\frac{\frac{3}{4}C^2 + \frac{3}{4}C - I(I+1)J(J+1)}{2I(2I-1)J(2J-1)} \quad \text{(Joules)} \qquad (11)$$

where E_J is the energy of the $n^{2S+1}L_J$ state, that is, the $5^2P_{3/2}$ or the $5^2S_{1/2}$ state shown in figure 4. From figure 4 note that in equation 11 for the $5^2P_{3/2}$ state I = 3/2, J = 3/2, and F′ = 0,1,2,3; and for the $5^2S_{1/2}$ state I = 3/2, J = 1/2, and F =1,2.

The frequencies $\nu_{J,F}$ (energy/h) of the various hyperfine levels are obtained by dividing equation 11 by Planck's constant h:

$$\nu_{J,F} = \nu_J + A\frac{C}{2} + B\frac{[\frac{3}{4}C(C+1) - I(I+1)J(J+1)]}{2I(2I-1)J(2J-1)} \text{(Hz)} \quad (12)$$

where $A \equiv \alpha/h$ and $B \equiv \beta/h$ have units of hertz.

For the $5^2S_{1/2}$ state of ^{87}Rb, the term that multiplies B in equation 13 reduces to zero and the accepted value of A is 3417.34 MHz. For the $5^2P_{3/2}$ state of ^{87}Rb, the accepted values of A and B are 84.85 MHz and 12.52 MHz, respectively. For the $5^2S_{1/2}$ of ^{85}Rb the accepted value of A is 1011.91 MHz, and for the $5^2P_{3/2}$ the accepted values of A and B are 25.01 MHz and 25.9 MHz, respectively.

Exercise 5.

For the $5^2S_{1/2}$ state of ^{87}Rb substitute numerical values for I, J, and F into the third term of equation 12 and show for both F = 1 and 2 that this formula only makes sense if B = 0 for these two cases.

Exercise 6.

For ^{87}Rb use equation 12 to show that: (1) for the $5^2S_{1/2}$ state the splitting of the F = 1 and F = 2 levels, $\nu_{1/2,2} - \nu_{1/2,1}$, is 6834.7 MHz, as shown in figure 3c, (2) for the $5^2P_{3/2}$ state the splitting of the F′ = 3 and F′ = 2 levels, $\nu_{3/2,3} - \nu_{3/2,2}$, is 267.1 MHz, as shown in

figure 3c, (3) the frequency spacing $\Delta\nu = \nu_{3/2,2} - \nu_{J=3/2}$ is 194.0 MHz, as shown in figure 4. (4) Now that you know how to do the calculations using equation 12, just use the energy level spacings given in figures 3 and 4 to shown the frequency of transitions a and b are $3.846 \times 10^{14} - 2.7933 \times 10^{9}$ Hz and $3.846 \times 10^{14} - 2.7147 \times 10^{9}$ Hz, respectively, hence the separation of these two spectral lines is 79 MHz. (5) Show that the frequency separation of spectral lines a and l is 6.993 GHz, and then show that their wavelength separation is 0.0142 nm.

One goal of this experiment is to experimentally determine A and B for the $5^2P_{3/2}$ state of ^{87}Rb.

Doppler Broadening and Absorption Spectroscopy

Random thermal motion of atoms or molecules creates a Doppler shift in the emitted or absorbed radiation. The spectral lines of such atoms or molecules are said to be Doppler broadened since the frequency of the radiation emitted or absorbed depends on the atomic velocities. (The emission spectral lines in both Experiments 12 and 13, reference 15, will be Doppler-broadened.) Individual spectral lines may not be resolved due to Doppler broadening, and, hence, subtle details in the atomic or molecular structure are not revealed. What determines the linewidth of a Doppler broadened line? To answer this question we do some theoretical physics.

We first consider the Doppler effect qualitatively. If an atom is moving toward or away from a laser light source, then it "sees" radiation that is blue or red shifted, respectively. If an atom at rest, relative to the laser, absorbs radiation of frequency ν_o, then when the atom is approaching the laser it will see blue-shifted radiation, hence for absorption to occur the frequency of the laser must be less than ν_o in order for it to be blue-shifted to the resonance value of ν_o. Similarly, if the atom is receding from the laser, the laser frequency must be greater than ν_o for absorption to occur.

We now offer a more quantitative argument of the Doppler effect and atomic resonance, where, as before, ν_o is the atomic resonance frequency when the atom is at rest in the frame of the laser. If the atom is moving along the z axis, say, relative to the laser with $v_z << c$, then the frequency of the absorbed radiation in the rest frame of the laser will be ν_L, where

$$\nu_L = \nu_o\left(1+\frac{v_z}{c}\right) \qquad (Hz) \quad (13)$$

If v_z is negative (motion toward the laser) then $\nu_L < \nu_o$, that is, the atom moving toward the laser observes radiation that is blue-shifted from ν_L up to ν_o. If v_z is positive (motion away from the laser) then $\nu_L > \nu_o$, that is, the atom observes radiation that is red-shifted from ν_L down to ν_o. Therefore, an ensemble of atoms

having a distribution of speeds will absorb light over a range of frequencies.

The probability that an atom has a velocity between v_z and $v_z + dv_z$ is given by the Maxwell distribution

$$P(v_z)\,dv_z = \left(\frac{M}{2\pi kT}\right)^{1/2} \exp\left(-\frac{Mv_z^2}{2kT}\right) dv_z \qquad (14)$$

where M is the mass of the atom, k is the Boltzmann constant, and T is the absolute temperature. From equation 13

$$v_z = (\nu_L - \nu_o)c/\nu_o; \qquad dv_z = cd\nu_L/\nu_o \quad (m/s) \quad (15)$$

Substituting (15) into (14), the probability of absorbing a wave with a frequency between ν_L and $\nu_L + d\nu_L$ is given in terms of the so-called linewidth parameter $\delta \equiv 2(\nu_o/c)(2kT/M)^{1/2}$ by

$$P(\nu_L)\,d\nu_L = \frac{2}{\delta\pi^{1/2}} \exp\left(-4(\nu_L - \nu_o)^2/\delta^2\right) d\nu_L \qquad (16)$$

The half width, which is the full-width at half maximum amplitude (FWHM), of the Doppler-broadened line is given by

$$\Delta\nu_{1/2} = \delta(\ln 2)^{1/2} = 2\frac{\nu_o}{c}\left(\frac{2kT}{M}\ln 2\right)^{1/2} \quad (Hz) \quad (17)$$

The profile of a Doppler-broadened spectral line is shown in figure 5. Substituting numerical values for the constants, equation 17 becomes

$$\Delta\nu_{1/2} = 2.92 \times 10^{-20}\nu_o\left(\frac{T}{M}\right)^{1/2} \qquad (18)$$

where M is the mass of the absorbing atom in kilograms and T is the absolute temperature in kelvins. So from equation 17 the FWHM of a Doppler broadened line is a function of ν_o, M, and T.

Exercise 7.

Show that the FWHM of the 780-nm spectral line of Rb at 297 K due to Doppler-broadening is 513 MHz.

The spectral absorption lines you will observe using absorption

spectroscopy will be Doppler-broadened. However, the absorption lines you will observe using saturated absorption spectroscopy will not be Doppler-broadened, in fact, they will approach the minimum or natural linewidth determined by the Heisenberg uncertainty principle.

Exercise 8.

For an atom with no Doppler shift, the linewidth is determined by the Heisenberg uncertainty principle, $\Delta E \approx h/\tau$, where τ is the excited state lifetime, and the range of frequencies absorbed is given by $\Delta\nu \approx 1/2\pi\tau$. From the expression for $\Delta\nu$ make a reasonable estimation of an expression for the FWHM, $\Delta\nu_{1/2}$, and using the 28-ns lifetime of the $^2P_{3/2}$ excited state of ^{87}Rb calculate the FWHM. Compare your answer to the 513 MHz FWHM in Exercise 7.

Exercise 9.

When you perform absorption spectroscopy on ^{87}Rb how many spectral lines do you predict will be resolved? To answer this question use the 513 MHz FWHM from Exercise 7 and use the spectral line separations that are given in figure 4.

Doppler-Free Saturated Absorption Spectroscopy

The setup for a classic Doppler-free saturated absorption spectroscopy of Rb is shown in figure 6. This isn't exactly the geometry we will use, but it most clearly illustrates the effects in nonlinear spectroscopy. The output beam from the laser is split into three beams, two less intense probe beams and a more intense pump beam, at the beamsplitter BS. The two probe beams pass through the Rb cell from left to right, and they are separately detected by two photodiodes. After being reflected twice by mirrors M1 and M2, the more intense pump beam passes through the Rb cell from right to left. Inside the Rb cell there is a region of space where the pump and a probe beam overlap and, hence, interact with the same atoms. This overlapping probe beam will be referred to as the first probe beam and the other one the second probe beam.

The signal from the second probe beam will be a linear, absorption spectroscopy signal, where the spectral lines will be Doppler-broadened. The signal is shown in figure 7a, and it was photographed from the screen of an oscilloscope. There are two Doppler-broadened lines shown in the 7a, and a portion of the triangular waveform that drives the PZT, and, hence sweeps the laser frequency, is also shown. The transition is the F = 2 to F' transition, and the larger amplitude signal is that of the 72% abundant ^{85}Rb and the smaller amplitude signal is that of the 28% abundant ^{87}Rb. This signal was obtained by blocking the pump and first probe beams.

If the second probe beam only is blocked then the signal from the first probe beam will be a nonlinear, saturated absorption spectroscopy signal "riding on" the Doppler-broadened line. This signal is shown in figure 7b, where the two Doppler-broadened lines

are the same transitions as in 7a, but note the hyperfine structure riding on these lines.

If the two signals in 7a and 7b are subtracted from each other, then the Doppler-broadened line cancels and the hyperfine structure remains. The two photodiodes shown in figure 6 are wired such that their signals subtract, and the signal obtained when none of the beams are blocked is shown in figure 7c for ^{87}Rb. In 7c note that the amplitude of the triangular waveform is one-fourth as large as in 7a and b, that is, in 7c the laser is being swept over a range that is one-fourth as large as in 7a and b. The signal shown in 7c is the Doppler-free saturated absorption signal. We now consider in detail the physics behind figure 7.

We start by focussing on the first probe and pump beams. The pump beam changes the populations of the atomic states and the probe detects these changes. Let us first consider how the pump beam changes the populations, and then we will discuss how these changes affect the first probe signal. As discussed above, because of the Doppler shift only atoms with a particular velocity v_z will be in resonance with the pump beam, and thereby be excited. This velocity dependent excitation process changes the populations in two ways, one way is known as "hyperfine pumping" and the other as "saturation". Hyperfine pumping is the larger of the two effects, and it will be discussed first.

Hyperfine pumping is optical pumping of the atoms between the hyperfine levels of the $5^2S_{1/2}$ state. This happens in the following manner. Suppose the laser frequency is such that an atom in the F = 1 ground state is excited to the F' = 1 excited state. The ΔF selection rule indicates that this state can than decay back to either the F = 1 or F = 2 ground states, with roughly equal probabilities. When it decays back to the F = 1 state it will be reexcited by the laser light and the process repeated. Thus after a very short time interval most of the atoms will be in the F = 2 state, and only a small fraction will remain in the F = 1 state. If the atoms never left the pump laser beam, even a very weak laser would quickly pump all the atoms into the F = 2 state. However, the laser beam diameter is small and the atoms are moving rapidly so that in a few microseconds the optically pumped atoms leave the beam and are replaced by unpumped atoms whose populations are equally distributed between the F = 1 and F = 2 levels. (You are ask to show below, in Exercise 10, that the populations of these two levels are essentially equal at room temperature with the laser turned off.) The average populations are determined by the balance between the rate at which the atoms are being excited and hence optically pumped, and the rate they are leaving the beam to be replaced by fresh ones. Without solving the problem in detail, one can see that if the laser intensity is sufficient to excite an atom in something like 1 microsecond it will cause a significant change in the populations of the F = 1 and F = 2 levels, that is, more atoms will be in the F = 2 level than the F = 1 level. This mechanism is called hyperfine pumping since the net effect is pumping electrons from the F = 1 ground hyperfine level to the F = 2 excited hyperfine level of

the $5^2S_{1/2}$ state. Although the example used was for the F = 1 to F′ = 1 transition, similar hyperfine pumping will occur for any excitation where the excited state can decay back into a ground state which is different from the initial ground state.

Exercise 10.

With the laser off, the ratio of the number of atoms in the energy level $E_{1/2,2}$ (J = 1/2, F = 2), $N(E_{1/2,2})$, to the number of atoms in the energy level $E_{1/2,1}$ (J = 1/2, F = 1), $N(E_{1/2,1})$, is determined by Maxwell-Boltzmann statistics:

$$\frac{N(E_{1\,2,2})}{N(E_{1\,2,1})} = \exp\text{-}\left(\frac{E_{1\,2,2} - E_{1\,2,1}}{kT}\right) \qquad (19)$$

Assuming a temperature of 295 K, show that the above population ratio is 0.999, hence the two levels are essentially equal populated with the laser off.

Exercise 11.

Show that laser excitations from F = 1 to F′ = 2, F = 2 to F′ = 1, and F = 2 to F′ = 2 will also produce hyperfine pumping of the $5^2S_{1/2}$ ground state, where the first excitation produces a larger population in the F = 2 than in the F = 1 level, and the other two excitations produce the larger population in the F = 1 level. Also show that laser excitations from F = 2 to F′ = 3 and F = 1 to F′ = 0 will not produce hyperfine pumping of the $5^2S_{1/2}$ state. One way to show the production, or nonproduction, of hyperfine pumping for each case is to show the upward transition and all of the allowed downward transitions on an energy level diagram like that in figure 3c, where the hyperfine levels of the $5^2P_{1/2}$ state do not need to be shown since we are not interested in transitions to these levels.

The other process by which the laser excitation to an excited F′ level changes the ground state population is known as saturation. It was pointed out in Exercise 10 that when an atom is excited to an F′ level it spends 28 ns in this level before it decays back to the ground state. If the pump beam intensity is low, it will stay in the ground state for much more than 28 ns before it is reexcited, and thus on the average almost all the atoms are in the ground state. However, if the pump intensity is high enough, it can reexcite the atom very rapidly. One might expect that if it was very high it would excite the atom in less than 28 ns. In this case most of the population would be in the excited state and very little would be left in the ground state. In fact, because the pump laser can "excite" atoms down just as well as up, this does not happen. For very high intensity a limit is reached where half the population is in the excited state and half is in the ground state. For realistic intensities the population of the excited state will be less than

0.5, something like 2 to 20 % is more typical. The effect of using high power to rapidly pump the atoms to an excited state is known as "saturating the transition" or just saturation. (In many references hyperfine pumping is also referred to as saturation.)

This saturation effect will be present on the transitions which have hyperfine pumping as well as the transitions which do not. However, it is generally a smaller effect than the hyperfine pumping. This can be understood by considering the intensity dependence of these two effects on the population. We previously indicated that the hyperfine pumping starts to become important when the excitation rate is about once per microsecond. From the discussion above, it can be seen that the saturation of the transition will become important when the excitation rate is comparable to the excited state lifetime, or once every 28 ns. Thus hyperfine pumping will occur at much lower intensities than saturation. The intensities you will be using are low enough that the hyperfine pumping will be substantially larger than saturation. This is also why the F = 2 to F′ = 3 and F = 1 to F′ = 0 signals are much smaller than the other transitions in the saturated absorption signals. As one increases the intensity these peaks will become larger relative to the other peaks for the same reason.

Summarizing, in the absence of laser light the F = 2 and F = 1 levels have nearly equal populations, and when the pump beam is on and tuned to either the F = 1 to F′ = 1, F = 1 to F′ = 2, F = 2 to F′ = 1, or the F = 2 to F′ = 2 transition, then hyperfine pumping produces a larger population in either the F = 1 or the F = 2 level.

We now ask, "How does the hyperfine pumping by the pump beam affect the first probe beam?" Well, in the arrangement of figure 6 imagine that all of the atoms in the Rb cell are at rest and consider what happens when the laser frequency ν_L is tuned to ν_o, the frequency of an atomic absorption line of the Rb atoms, for example, the F = 1 to F′ = 1 transition. The hyperfine pumping by the more intense pump beam produces a smaller population in the F = 1 level than that in the F = 2 level. This means there are fewer atoms in the F = 1 level that will absorb power from the first probe beam, hence the number of photons in the first probe beam that reach the photodiode detector will increase. Now the second probe beam is interacting with a different group of atoms in the vapor cell, hence it is not influenced by the pump beam; therefore, the second probe beam's intensity at its photodiode detector will be less than that of the first probe beam. Hence, the intensity of the two probe beams that both drive transitions from the $5^2S_{1/2}$ hyperfine levels to the $5^2P_{3/2}$ hyperfine levels will be different, and thus even after subtracting the two signals in the current-to-voltage converter, the resulting signal will show power absorption due to driving transitions between these levels. Also both probe beams will be Doppler broadened, and subtracting them eliminates the Doppler-broadened line as shown in figure 7c.

The atoms in the vapor cell will, of course, not all be at rest; instead they will have a distribution of velocities given by

equation 11, the Maxwell distribution. An atom that absorbs light at frequency ν_o, when at rest, will absorb laser light of frequency ν_L, where ν_L is given by equation 13, when the atom moves with velocity $\pm v_z$ along the axis of the vapor cell. Consider the Maxwell distribution of atomic velocities shown in figure 8, where the number of ground state atoms $N_{gs}(v_z)$ is plotted against the atom velocity v_z.

The positive z axis is arbitrarily chosen in the direction of the probe beams. We will consider the three cases of figure 8 in order.

(a) $\nu_L < \nu_o$. Atoms moving toward the right are moving toward the pump beam and they will see its light blue-shifted. At appropriate positive v_z (equation 13), the light will be shifted to ν_o in the rest frame of the atoms, where ν_o is the frequency of a transition from an F level to an F' level. Atoms moving at this velocity v_z will absorb the pump laser light. The probe beam is moving to the right, hence atoms moving to the left with the same velocity magnitude will absorb the probe beams. It is important to recognize that the three beams are interacting with three different groups of atom. The two probe beams are interacting with atoms in different regions of the vapor cell moving to the left with velocity v_z, while the pump beam is interacting with atoms moving to the right with velocity v_z. Also the more intense pump beam causes a greater reduction in the number of atoms in the ground state than the less intense probe beams as is shown in figure 8a. Subtraction of the two probe beams gives a null signal.

(b) $\nu_L = \nu_o$. Atoms with speed $v_z = 0$ in the region of overlapping first probe and pump beams can absorb light from both the first probe and pump beams. For the F = 1 to F' = 1 transition, for example, the pump beam depletes the population of the F = 1 level, and then the first probe beam passes through with reduced absorption. Reduced absorption of the second probe beam does not occur, hence subtraction of the two signals gives an absorption signal without Doppler broadening. The interaction is nonlinear in that the first probe signal depends upon the fields of both the first probe and pump beams.

(c) $\nu_L > \nu_o$. This is like (a) with directions reverse, and subtraction of the two probe beam signals gives a null result.

A crossover transition occurs when the laser frequency is halfway between two transitions that share a common ground state, for example, the F = 2 -> F' = 3 transition and the F = 2 -> F' = 1 transition. When the laser frequency is at the midpoint between two such frequencies, then a group of atoms having the appropriate velocity will see the probe beams blueshifted to the F = 2 -> F' = 3 transition and the pump beam redshifted to the F = 2 -> F' = 1 transition. Also another group of atoms will see the opposite Doppler shifts of the probe and pump beams that results in a crossover resonance at the same frequency. In both cases the pump beam reduces the population in the F = 2 level, which results in an increased transmission of the probe beam that overlaps with the pump

beam. Note that for each crossover resonance the absorption is saturated not by stationary atoms but by two classes of moving ones.

Experiments

Setup: A less classic, but simpler setup for saturated absorption spectroscopy is shown in figure 6b. This is the setup currently in use for the atom trap experiment. As shown in the figure, there is not a separate pump beam, instead one of the probe beams retraces its path through the Rb cell. In this way it acts as both probe and pump. Saturated absorption features will be seen in the absorption spectrum of this beam. Also shown in 6b is a Fabry-Perot interferometer to measure the frequency changes.

New Focus Grating-Tuned Diode Laser: This laser system consists of two parts: the Controller, which has all the adjustment knobs and indicators, and the Laser Head, which contains a laser diode. The laser diode is a semiconductor light amplifier. Electrons and holes meet annihilate in the diode to produce photons. The presence of other photons accelerates this process (by stimulated emission), so the diode acts as a photon amplifier. Also in the laser head is a diffraction grating, placed so that a certain wavelength, when emitted by the laser, is diffracted back at the laser. Photons of this wavelength bounce repeatedly between the grating and the diode being amplified on each pass through the diode. Any other wavelength will diffract off the grating at a slightly different angle and will miss the diode. In this way the angle of the grating determines the wavelength of the laser light. Other factors also influence the wavelength: diode temperature, temperature of the laser head, current through the diode and mechanical vibrations. To tune the laser, all these other factors will be held as constant as possible while the grating is rotated slightly with a piezo-electric transducer (a PZT).

The laser controller should already be on. If it is not, turn it on using the key and wait until the temperature has stabilized. Don't adjust the temperature, just wait for it to reach a steady value. Start by turning the diode current to zero. Then press the Laser Power button. Slowly turn up the laser current. At around 40 mA you should be able to see (using the IR card, not by eye) some light emanating from the laser head. At around 60 mA there should be a clear beam and the controller should register both power and wavelength of the laser. Adjust the laser current to get 4 mW of laser power. Under no circumstances should the laser current exceed 80 mA. The laser wavelength should read something near 780.02 nm. If it does not, turn "tracking" on and adjust the wavelength. In "tracking" mode the controller tries to set the laser wavelength. This is good for getting close to the right wavelength, but once that's done you should turn off "tracking" so that the controller doesn't fight the tuning you will do with the PZT.

Using the IR card, follow the laser beam through the system.

Please don't adjust, bump, or otherwise disturb: the laser head itself, the half-wave plate, the prisms, or the beamsplitter. Movement of any of these will upset the alignment of other experiments using this laser such as the atom trap. If it is not already aligned, make the necessary adjustments so that both beams pass through the cell and that one of them is saturated. Each beam should reach a detector.

New Focus "Nirvana" photodetector:
This is actually two photodetectors and the circuitry to subract their signals. The "signal" output indicates the power reaching the "SIGNAL" detector. The "linear" output indicates one of several things. Set the linear selector to "Bal" for "balanced." On this setting the linear output will indicate the difference in power between "SIGNAL" and "ref" (reference) detectors.

Doppler-broadened spectrum:

To align to the detector: send both signal and linear outputs to the oscilloscope. Block the signal detector, and maximize the power at the reference detector by moving the detectors (not the beamsplitter). This should be well enough aligned to find the absorption resonances.

Laser wavelength modulation: Use a function generator to 1) trigger the oscilloscope and 2) generate a triangle wave of about 1 volt amplitude at about 100 Hz. Send the triangle wave to the "frequency modulation" input on the back of the diode laser controller. The PZT display on the controller should flicker, indicating that you are driving the PZT, which rotates the grating and thus changes the laser output frequency. If the laser head makes clicking or buzzing noises, you probably have the "tracking" enabled and the controller is trying to undo your frequency sweeps. Turn off the "tracking."

You may, at this point, already see a Doppler broadened spectrum on the oscilloscope. If not, try using the DC offset on the function generator to hunt for the spectrum.

Recording a spectrum:
The oscilloscope can save individual traces. Hit the "Stop" button to capture the most recent trace. With the GPIB interface and a computer, you can record the trace to disk and later print it out.If there is a GPIB-capable printer, you can print the spectrum directly via GPIB. With the oscilloscope's cursors you can easily measure points on the spectrum such as peaks and half-height points.

Once you have found the spectrum, record it, find the relative positions of the four Doppler-broadened peaks and identify them.

Which direction is higher frequency on your spectrum?

Doppler-Broadened Line with Hyperfine Structure

Once you have an absorption signal, look at the cell with the handheld IR viewer. You should be able to see the fluorescence of the rubidium vapor as the beam passes through the cell. Check that the double-pass beam overlaps itself as it returns through the cell.

Unblock the "SIGNAL" detector and maximize the power to it by adjusting the last mirror before the detector. You should observe a Doppler-broadened line with hyperfine structure riding on it, somewhat like that shown in figure 7b. Record the observed signal.

Doppler-Free Saturated Absorption Spectral Lines

With light hitting both detectors, the "linear" output of the photodetector should show the difference of the two detector signals. If the beams are equal power, this should be just the effect of saturation, i.e., the saturated absorption spectrum. The easiest way to adjust the power levels is to misalign each beam slightly so that most but not all of the power is reaching the detector. Then fine adjustments of the mirror alignment can balance the power levels. When the power is balanced, the Doppler-broadened spectrum should disappear, leaving just the saturation dips. Zoom in on the F=2 to F' = 1,2,3 transition by reducing the triangle-wave amplitude. You should see six dips as in Figure 7c. Record the spectrum and find the relative positions of the six dips. Now tune the laser, as described above, to the other transition, that is, if you have been studying the F = 2 to F' transition of ^{87}Rb tune the laser to the F = 1 to F' transition and record similar data.

Calibration of the spectrum:

The wavelength or frequency scale of the spectrum (which is the time axis on the scope) needs to be calibrated. For that you need an independent measure of frequency changes in the laser. For example, if you had a Fabry-Perot interferometer of length d=1 meter, its transmission maxima would be regularly spaced in frequency with a separation of $\Delta f = c/2d = 150$ MHz. As you scanned the laser frequency the interferometer transmission would show a comb of peaks, good for calibrating the frequency scale. One interferometer geometry is shown in Figure 6b.

Other ways to get an absolute measure of the frequency scale would be to use an optical spectrum analyzer, build a Michelson interferometer, or determine the positions of the rubidium absorption peaks using some other instrument, for example a high-resolution grating spectrometer.

Use your calibration technique to find the frequency difference

between the two most widely separated peaks on the Doppler-broadened spectrum. Also find the separation between the two most widely separated peaks on your saturated absorption spectrum. Record the traces.

Data Analysis

1. Measure the FWHM for each of the two Doppler-broadened lines of ^{87}Rb. Compare your values with your calculated value from Exercise 7.

2. Measure the frequency separation of the hyperfine lines for the F = 2 to F′ transitions, use equation 12 to obtain a theoretical expression for the frequency separation of the hyperfine lines, and then solve for the constants A and B for the $5^2P_{3/2}$ state of ^{87}Rb. Compare your results with the accepted values given earlier.

3. Measure the linewidth of one of the hyperfine lines and compare it with the natural linewidth calculated in Exercise 8. Our spectroscopic technique cleverly escapes (linear) Doppler broadening, but there are other, weaker, broadening mechanisms which remain. A) Collisional broadening is the result of collisions between the rubidium atoms or between rubidium and other gases in the cell. B) Power brodening results when the laser is intense enough to saturate the atomic absorption. C) Transit broadening is a consequence of the uncertainty principle: if an atom crosses the laser beam in a time $_{\Delta}t$, the energy can only be determined with a precision $_{\Delta}E = hbar/2_{\Delta}t$. D) The motion of an atom perpendicular to the laser beam has a small (proportional to v^2/c^2) effect on the transition frequency.

Exercise 12.

Knowing the natural and experimental linewidths determine the contribution to the linewidth produced by other broadening mechanisms. Could these other effects be reduced? How?

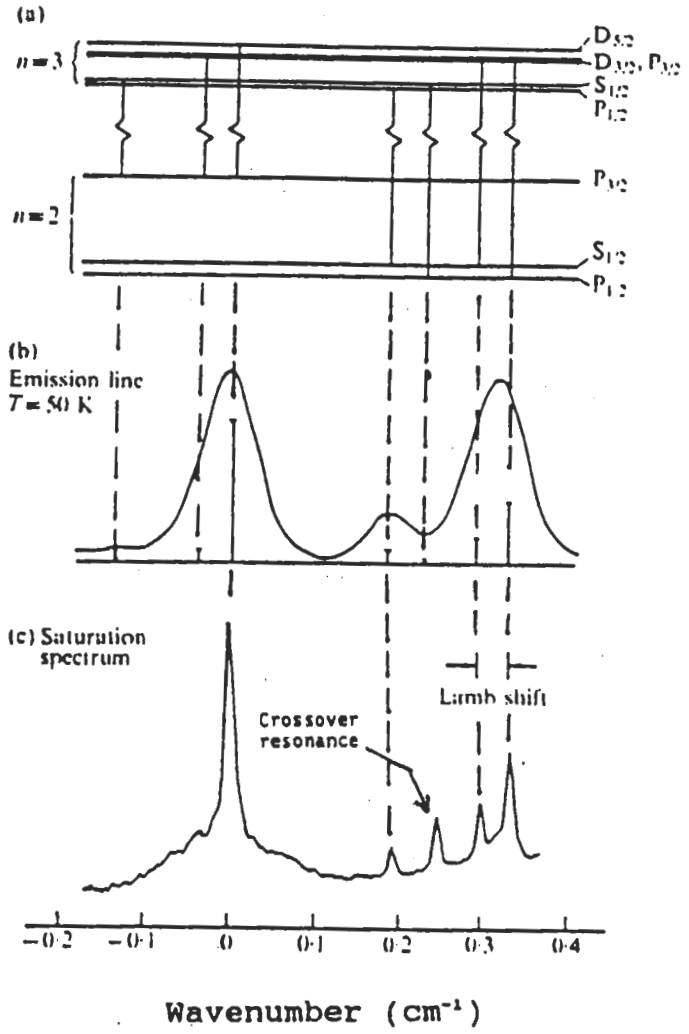

Figure 1. The Balmer α line of atomic deuterium: (a) Energy levels and allowed transitions, (b) the emission spectrum, (c) an early saturated absorption spectrum.

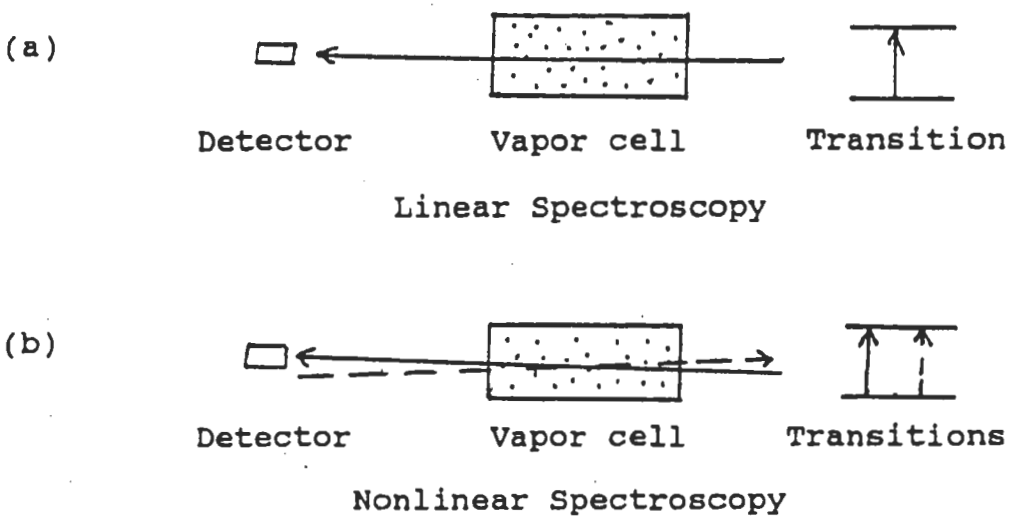

Figure 2. In linear spectroscopy (a) the radiation reaching the detector is proportional is the radiation incident on the sample, and in nonlinear spectroscopy (b) the radiation reaching the detector is dependent on both beams.

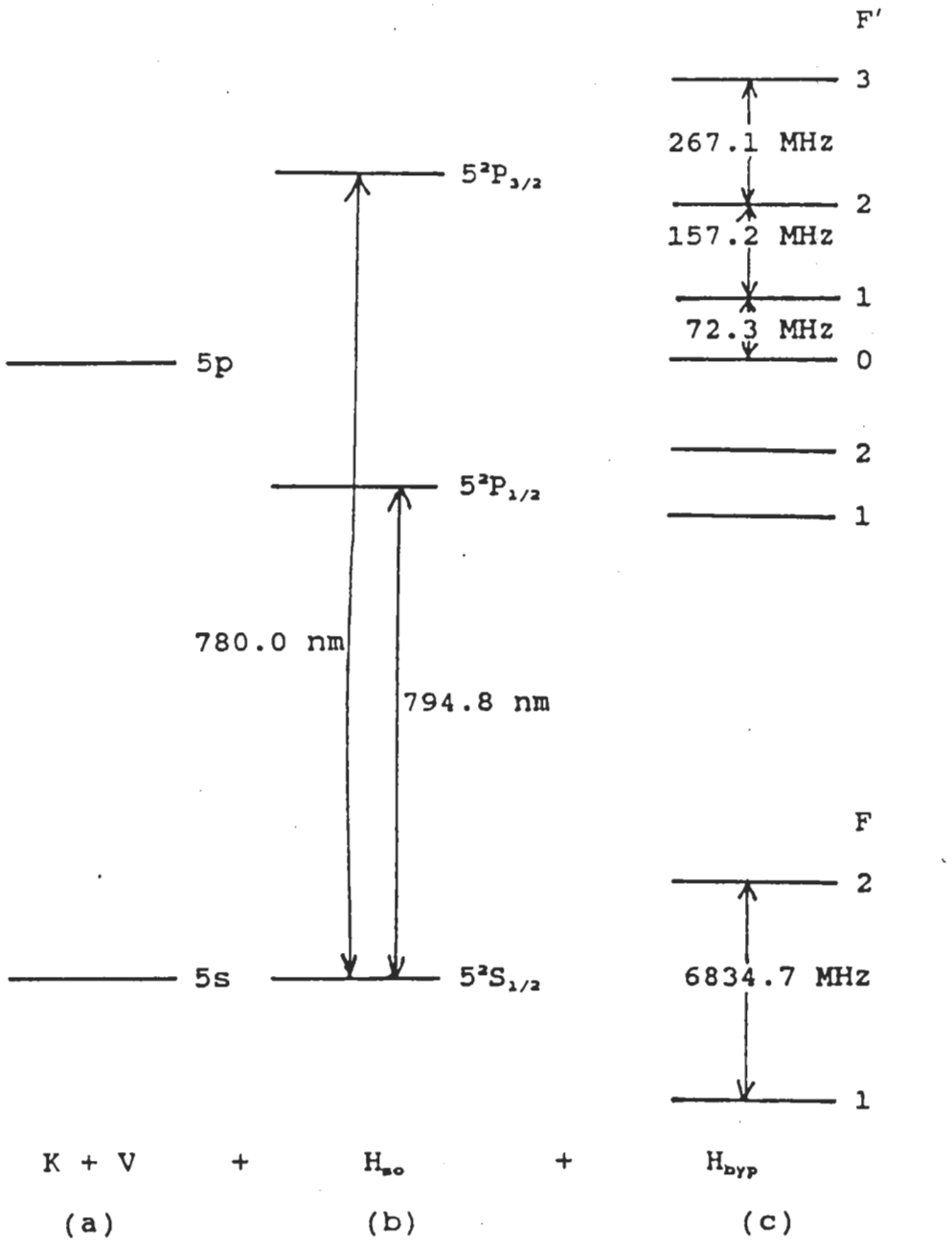

Figure 3. Each interaction in equation 6 and its effect on the energy levels of the 5s and 5p electron is shown. The energy level spacings are not to scale. The hyperfine levels are for ^{87}Rb.

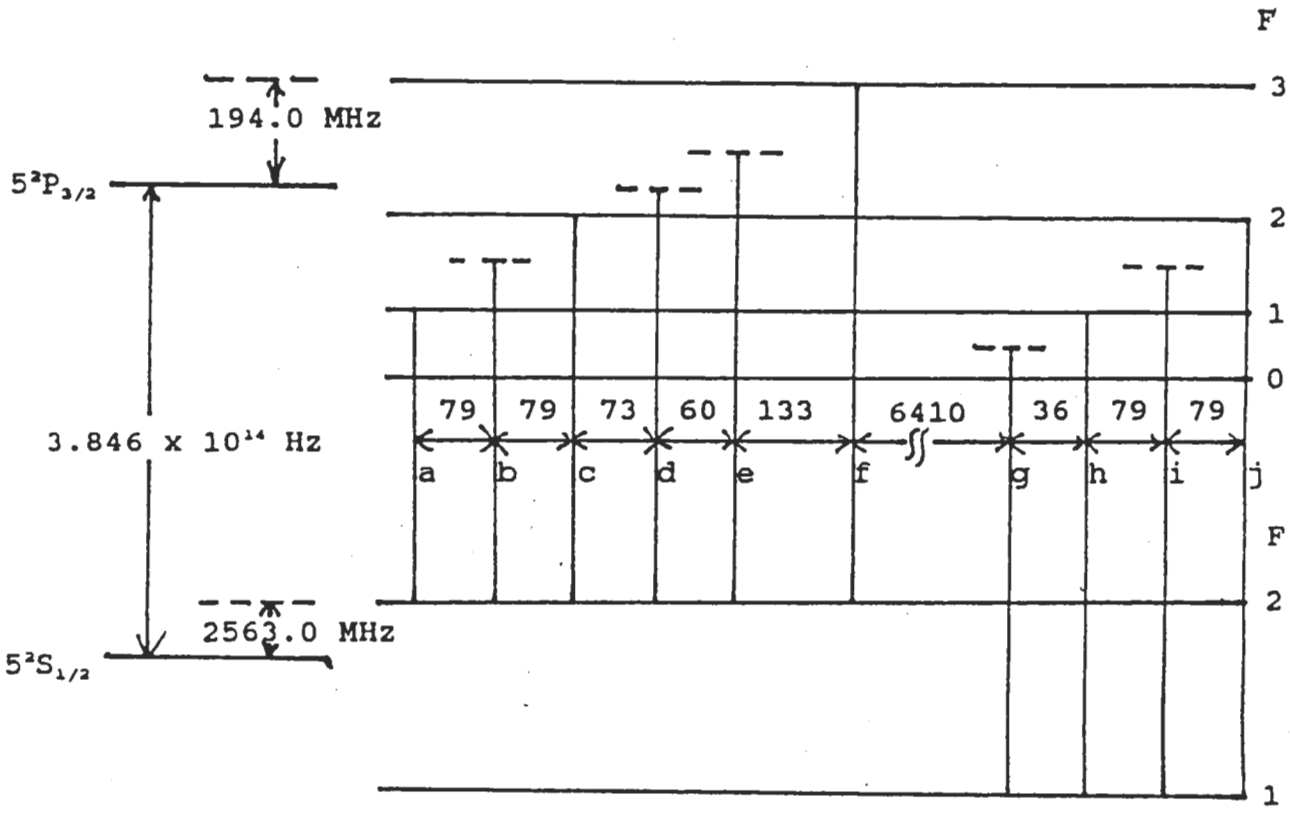

Figure 4. Saturated absorption transitions for ^{87}Rb. The spectral line separation, 79, 79, etc., is in MHz.

[37]G. J. Chaitin, "Incompleteness theorems for random reals," Adv. Appl. Math. 8, 119–146 (1987).
[38]S. Wolfram, "Undecidability and intractability in theoretical physics," Phys. Rev. Lett. 54, 735–740 (1985).
[39]E. Fredkin and T. Toffli, "Conservative logic," Intl. J. Theor. Phys. 21, 219–232 (1982).
[40]D. Ornstein and B. Weiss, "Statistical properties of chaotic systems," Bull. Am. Math. Soc. 24, 11–116 (1991).

A narrow-band tunable diode laser system with grating feedback, and a saturated absorption spectrometer for Cs and Rb

K. B. MacAdam,[a] A. Steinbach, and C. Wieman
Joint Institute for Laboratory Astrophysics and the Department of Physics, University of Colorado, Boulder, Colorado 80309-0440

(Received 6 February 1992; accepted 26 June 1992)

Detailed instructions for the construction and operation of a diode laser system with optical feedback are presented. This system uses feedback from a diffraction grating to provide a narrow-band continuously tuneable source of light at red or near-IR wavelengths. These instructions include machine drawings for the parts to be constructed, electronic circuit diagrams, and prices and vendors of the items to be purchased. It is also explained how to align the system and how to use it to observe saturated absorption spectra of atomic cesium or rubidium.

I. INTRODUCTION

Tuneable diode lasers are widely used in atomic physics. This is primarily because they are reliable sources of narrow-band (<1 MHz) light and are vastly less expensive than dye or Ti-sapphire lasers. However, the frequency tuning characteristics of the light from an "off the shelf" laser diode is far from ideal, and this greatly limits its utility. In particular, the laser output is typically some tens of MHz wide and can be continuously tuned only over certain limited regions. These characteristics can be greatly improved by the use of optical feedback to control the laser frequency. Reference 1 gives a lengthy technical review of the characteristics of laser diodes, the use of optical feedback techniques to control them, and various applications in atomic physics. An earlier review by Camparo[2] also gives much useful information, primarily relating to free-running diode lasers. The use of a wavelength-dispersive external cavity for diode laser tunning and mode selection was described by Ludeke and Harris,[3] and the spectral characteristics of external-cavity stabilized diode lasers were investigated in detail by Fleming and Mooradian.[4]

During the past several years our laboratory has carried out a large number of experiments in optical cooling and trapping, and general laser spectroscopy of cesium and rubidium using diode lasers. In the course of this work, we have developed a simple inexpensive design for a diode laser system that uses optical feedback from a diffraction grating. This system produces over 10 mW of light with a bandwidth of well under 1 MHz and can be easily tuned over atomic resonance lines. We now have over a dozen such laser systems operating, including two in an undergraduate teaching lab, and the design has reached a reasonable level of refinement. There are many other designs for optical feedback systems[1] and we make no claims for this one being superior. However, it is a reasonable compromise between several factors which are relevant to many laboratories: (1) low cost (about $400 not including labor), (2) ease of construction (several of these systems have been built by novice undergraduates), and (3) reliability. These lasers have achieved several notable successes in experiments on cooling and trapping cesium atoms, and the design has been successfully duplicated in a number of other laboratories. We prepared this article in response to a large number of requests for detailed instructions on how to build and operate such a system. This article provides a detailed and fully comprehensive recipe for construction of the system and its use to observe saturated absorption spectra in a rubidium or cesium vapor cell. We refer the reader to Ref. 1 and the references therein for information about the physics of laser diodes and the factors that motivated this design as well as design alternatives.

In this paper, we have attempted to respond to three frequent requests for information we receive. The first is from the undergraduate wanting to do high-resolution laser spectroscopy for a project, without expert local supervision. The second is from the faculty member who wants to construct a teaching laboratory experiment and wants instructions that can be given to a technician or undergraduate with favorable results. The third is from the research scientist who wants to use diode lasers in an experiment and would like to benefit from the accumulated practical experience in another laboratory.

We will first discuss the construction or purchase of the basic components and then explain how to put them together, align the laser system, and tune the frequency. Finally, we discuss how to observe saturated absorption spectra and how to use these spectra to evaluate the laser performance or to actively stabilize the laser frequency by locking it to narrow saturated absorption features.

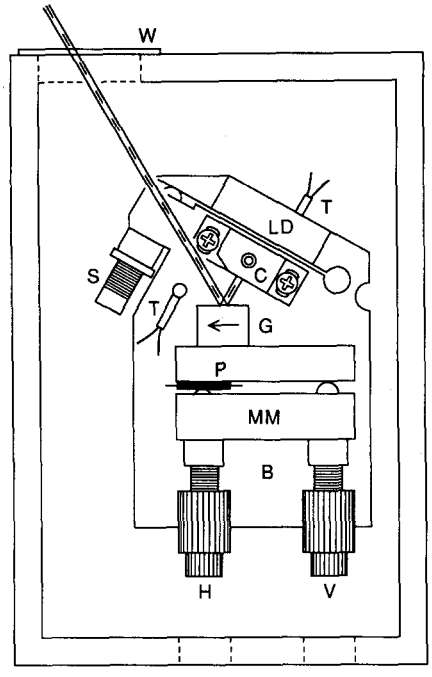

Fig. 1. Assembly top view of laser. The arrow showing the blaze direction on the grating is for the low feedback-large output case.

II. SYNOPSIS OF COMPONENTS

As shown in Fig. 1, the laser system has three basic components, a commercial diode laser, a collimating lens, and a diffraction grating. These components are mounted on a baseplate. The laser and lens are mounted so that the lens can be carefully positioned relative to the laser to insure proper collimation. The diffraction grating is mounted in a Littrow configuration so that the light diffracted into the first order returns to the laser. As such, the grating serves as one end "mirror" of a laser cavity, with the back facet of the diode providing the second mirror. This means the grating must be carefully aligned and very stable. To achieve this we mount the grating on a standard commercial mirror mount which is attached to the baseplate. As with any laser, changes in the length of the cavity cause shifts in the laser frequency. Therefore, to obtain a stable output frequency, undesired changes in the length due to mechanical movement or thermal expansion must be avoided. To reduce movements due to vibration of the cavity we mount it on small soft rubber cushions. To avoid thermal changes, the baseplate is temperature controlled using heaters and/or thermoelectric coolers. In addition to controlling the temperature of the baseplate, we independently control the temperature of the laser diode. Finally, to avoid air currents interfering with the temperature control we enclose the entire laser system in a small insulated metal box. Of course, to finely tune the laser frequency one must have some way to change the length of the cavity in a carefully controlled manner. We do this using a piezoelectric transducer speaker disk which moves the grating in response to an applied voltage.

The laser system also requires a small amount of electronics. A stable low-noise current source is needed to run the laser, and temperature control circuits are used to stabilize the diode and baseplate temperatures. This electronics is readily available commercially. However, for those with more time than money, we provide circuit diagrams for the relatively simple circuits that we normally use.

This system contains both purchased and "homemade" components. Before discussing the construction aspects, we will provide some information concerning the purchasing of the commercial components. We purchase the diode laser itself, the collimating lens, the fine adjustment screw which controls the lens focus, the diffraction grating, the mirror mount which holds the grating, and the piezoelectric disks. The purchase of most of these items is straightforward. Fine adjustment screws and mirror mounts are available as standard items from most companies that sell optics hardware. Similarly, laser diode collimating lenses and diffraction gratings are available from numerous companies. For the convenience of the reader we list in the Appendix the exact products we use along with the prices and vendors. However, for these items our choice of vendors was primarily determined by expediency, and we have no reason to think that other vendors would not provide equal or superior products.

In contrast, in order to obtain satisfactory laser diodes and piezo disks we have tried and rejected a large number of different vendors. Piezo disks are widely sold as electronic speakers and are very inexpensive, but most models are not adequate for this application. The Appendix gives the only suitable product we have found. The purchasing of diode lasers can be filled with frustrations and pitfalls, and we refer the reader to Ref. 1 for a full discussion of the subject. Here, we shall just give a brief summary of what must be specified, and our recommendations for suppliers. The basic requirement for a diode laser which is to be used in this system is that it have a high reflectivity coating on the back facet and a reduced reflectivity on the front, or output facet. Very inexpensive diodes which produce a few milliwatts of power have two uncoated facets, and will not work very well. We have used 20-mW lasers, but their performance is marginal. However, we have found that any laser we have tried that is specified to provide 30 mW or more single mode will have the necessary coatings and will work well.[5] It will provide narrowband laser light that is tuneable over 20–30 nm. If one wants this range to cover the 852-nm cesium or 780-nm rubidium resonance lines, the diode laser wavelength must be specified when purchasing. This greatly complicates the purchasing. We have tried numerous suppliers, but have now settled on STC as our supplier of lasers for 852 nm and Sharp as the supplier for 780 nm. The Sharp lasers are far less expensive and can usually be obtained rather quickly since 780 nm is near the center of the distribution of their normal mass-produced product. This is not the case for 852 nm, and thus the lasers must be produced as a custom run. STC has made several such custom runs and hence usually has 852-nm lasers available although they cost 3 to 4 times more than the Sharp lasers. The long wavelength edge of the distribution of Sharp lasers is at about 839 nm, and we have used such lasers to reach the cesium line by heating them. However, it can be difficult to obtain 839-nm lasers and to obtain reliable performance when tuning the laser this far from its free-running wavelength. The heating of the laser also degrades its lifetime.

The remaining components of the laser system are homemade. The key components are the laser mounting block which holds the actual diode laser, the holder for the collimating lens, and the baseplate onto which all the com-

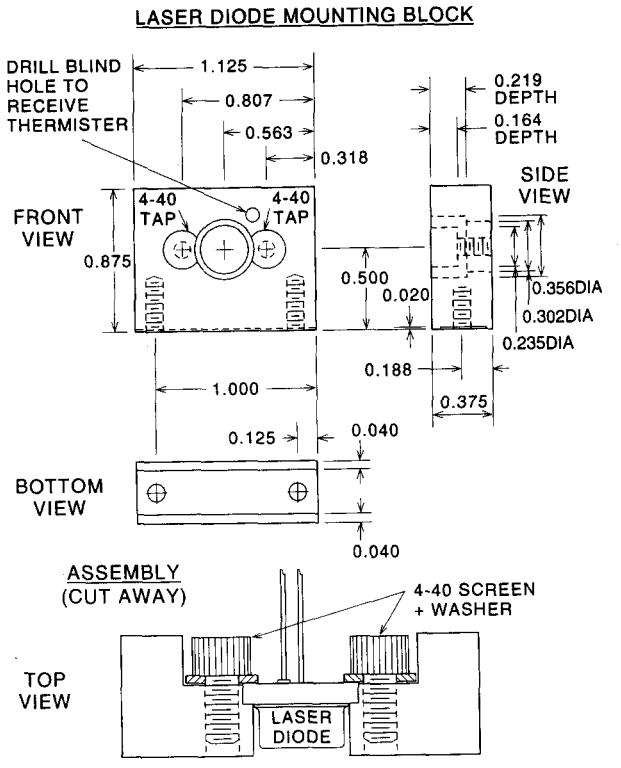

Fig. 2. Laser mounting block, machine drawing. Dimensions are in inches. The hole sizes, spacings, and depths are correct for a Sharp LT025MDO laser and may be modified for other types.

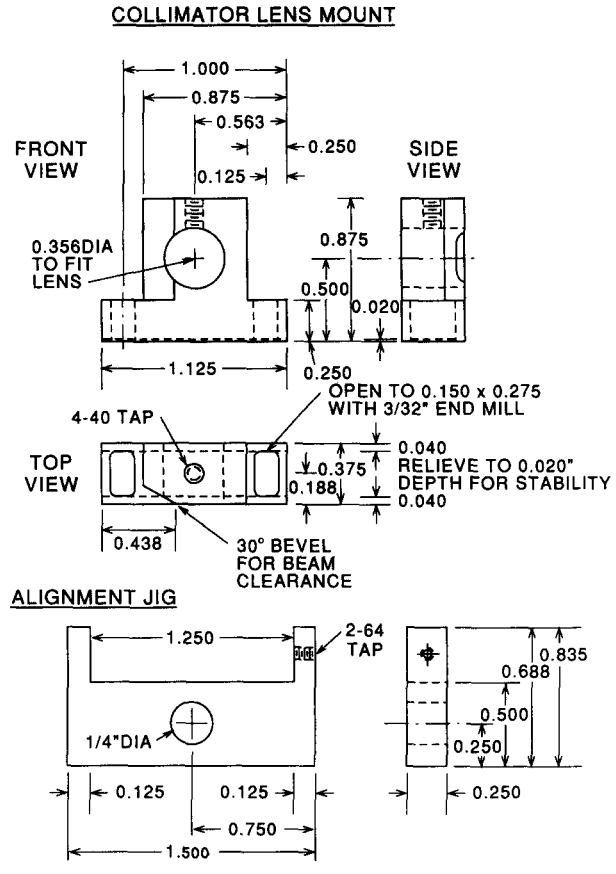

Fig. 3. Collimating lens mount and alignment jig machine drawing. Dimensions are in inches.

ponents are fastened. In addition, we also make the box that encloses the system and a small jig that is useful for setting the position of the collimating lens. All these components have been designed so that they can be constructed by a novice machinist.

III. INSTRUCTIONS FOR CONSTRUCTION OF LASER COMPONENTS

Construction of the diode laser system begins in the machine shop and primarily requires a milling machine and drill press. Detailed machine drawings for the laser mounting block, baseplate, collimating-lens holder, and an alignment jig are given in Figs. 2 and 3. In addition, an enclosure should be fabricated, but its design is not critical. We provide dimensions for mounting the standard Sharp laser package. Small changes may be needed for lasers from other vendors. In view of the setup time required in machining, and the fact that many interesting experiments with diode lasers require more than one of them, it will probably be found economical to make two (or more) systems at once.

A. Laser mounting block

The laser diode is held firmly in a small aluminum block whose details are shown in Fig. 2. The critical dimensions are the 0.500-in. height of the laser center above the baseplate and the depths of holes that ensure that the 9-mm flange of the diode package is gripped by the mounting screws. For stability when the block is screwed down to the baseplate, the bottom surface of the block should be machined as shown with a 0.020-in. relief cut down the middle so that contact is along the edges of the block. This "bridge" design has been found to make a significant improvement on laser cavity stability. The 0.356-in. diam hole to receive the diode package may be made either by boring on a lathe fitted with a four-jaw chuck or, more easily, by a suitable end mill. Reground 3/8-in. end mills can often be found near this diameter. Some deburring or filing may be necessary to allow the diode to fit snugly into its recess but allow it to be rotated to its proper orientation in the initial step of alignment. A small hole whose diameter is selected to fit the thermistor should be drilled into the back side of the mounting block near the diode recess.

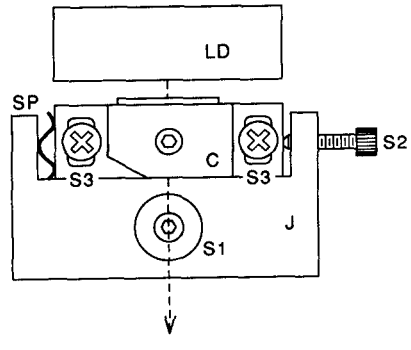

Fig. 4. Jig usage in collimation. LD=laser mounting block (Fig. 2), C=collimating lens mount (Fig. 3), J=alignment jig (Fig. 3). SP =spring or rubber pad to provide a restoring force against adjusting screw $S2$.

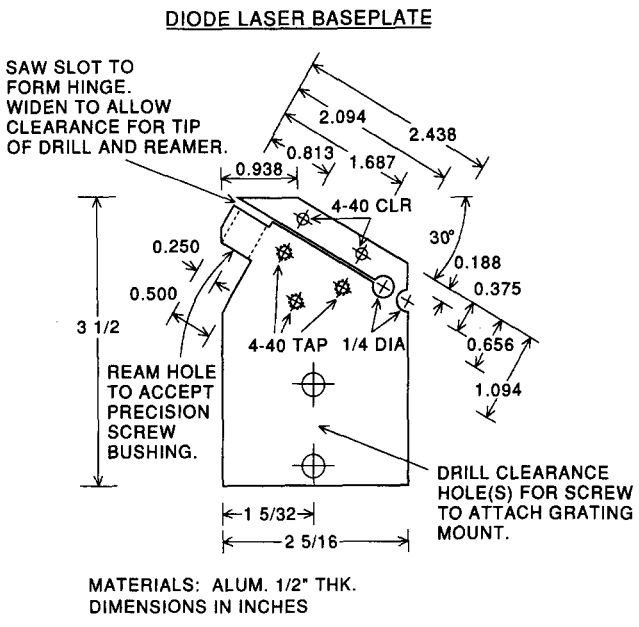

Fig. 5. Laser baseplate, machine drawing.

B. Collimator lens mount

Figure 3 shows the aluminum block that holds the flanged collimator lens. The placement of the lens axis at 0.500 in. above the base and the diameter of the hole are again the critical dimensions. The 30° bevel shown on the front side of the block allows clear passage of the output beam off the diffraction grating when very short cavities are used. The figure also shows dimensions of a suggested alignment jig that is used to allow transverse displacement of the lens holder without rotation or longitudinal movement. A 2-56 screw with rounded tip and a small piece of bent spring steel or resilient cushion should be prepared for use with the jig (as shown in Fig. 4).

C. Baseplate

The baseplate is shown in Fig. 5. We have found that aluminum is adequate for most purposes and is easy to machine. If greater thermal stability is required, however, the baseplate can be made of invar. The two pairs of 4-40 holes should be carefully positioned to match corresponding holes in the laser and collimator-lens blocks. The single 4-40 tapped hole is used to mount the alignment jig. The most obvious feature of the baseplate is its flex hinge design, which allows smooth variation of the spacing between diode and collimation lens by action of a commercial precision screw mounted to push against the hinge. The slot that forms the hinge can be cut by a bandsaw after all holes are laid out. The hole intended to receive the precision adjusting screw should be reamed to allow a fit without excess clearance. After all machining of the baseplate is complete the screw can be mounted in this hole with adhesive or by a set screw. The web that provides the flexible hinge should be left 1/16 in. or more in width: One can always remove material later if it proves too stiff. One or more holes should be drilled in the baseplate to mount the diffraction grating holder, but the exact position(s) depends on the dimensions of the holder and grating and on the desired cavity length. Several suitable holes drilled at this time will allow comparison of laser performance with different cavity lengths without complete disassembly of the collimated laser.

D. Grating and grating mount

The baseplate design is intended for use with a 1200 line-per-mm grating. Suitable gratings are readily obtained with 500- and 750-nm blazes and dimensions $1\times1\times3/8$ in. thick. When mounted, the grating has its rulings vertical and diffracts its first-order interference maximum back into the laser. The output beam is the zero-order beam or specular-reflection maximum, which passes horizontally beside the collimator block and out of the enclosure. The direction of the blaze is toward the output beam. A laser diode whose free-running wavelength is within about 3 nm of the desired wavelength requires less feedback for stabilized operation than a laser that must be pulled more severely. For this case, lower diffraction efficiency and thus a shorter blaze wavelength (500 nm) is suitable, and this allows more power to be brought out in the zero-order beam. If a laser must be pulled more severely, a longer blaze wavelength (750 nm) is used to provide stronger feedback at the price of lower output power.[6]

When a grating of suitable blaze has been selected it may be cut down to a small size since only about 0.3 in. parallel to the rulings and 0.5 in. perpendicular is required. Thus several gratings can be had for the price of one, and the others may be used to duplicate the diode laser system or for testing grating properties outside the laser. The cutting may be safely done as follows. Apply a generous coating of clear acetate fingernail polish to the ruled face of the grating. Spread the fluid using a soft camel's hair brush, and avoid physical contact with the grating. After the coating is thoroughly dry, wax the back of the grating to a block of bakelite or phenolic to support the grating while it is sawed. Mark the coated surface of the grating into pieces of the desired size. A 1×1 in. grating will yield six suitable pieces. Saw the grating in an abrasive-wheel glass saw by holding the support block on its edge as the saw cuts directly into the face of the grating. Make sure the saw cuts penetrate completely through the grating into the support block without severing the block. Then melt off the cut segments. The nail polish can then be removed by submerging the grating segments in a small beaker of methanol and placing the beaker in an ultrasonic cleaner. Remove the gratings with tweezers, being very careful to avoid any contact with the now-exposed ruling surface, refill the beaker with fresh methanol, and repeat once or twice until the gratings, when drained and dried, appear completely clean. Harsher solvents may attack the plastic substrate of replica gratings, but methanol has been found to be safe and effective.

After cleaning, the grating is attached to the movable face of the grating mount in a location where the collimated laser beam will strike near the middle of the grating. Care should be taken to make the rulings vertical. A stiff but readily removable adhesive such as Duco cement is recommended for attaching the grating to the mount. The grating segment can be easily damaged when it is necessary to remove it or shift its position unless it can be detached with little physical force. If necessary, the efficiency of most inexpensive gratings at the 852-nm wavelength for Cs can be improved by 10%–20% by evaporating a gold coating onto the grating before it is installed.[7]

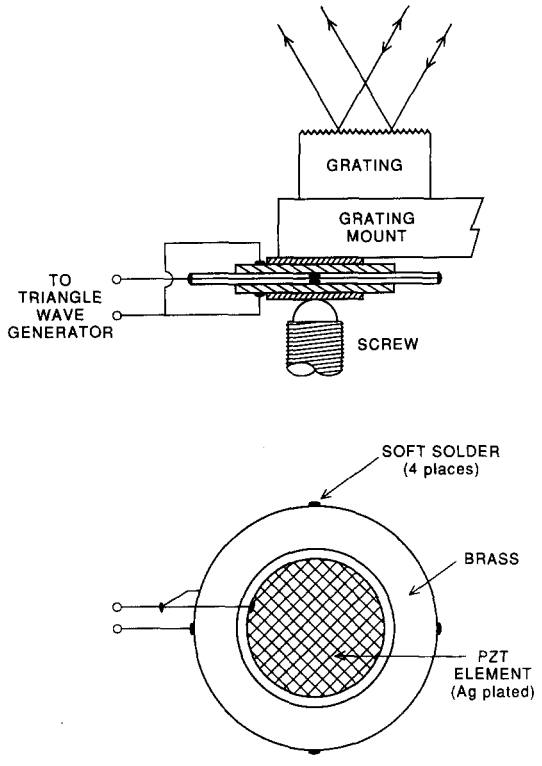

Fig. 6. Piezoelectric disks (not to scale).

Before the grating is attached to the mount, the mount should be modified, if necessary, so that it has the same "bridge" profile on its base as described earlier. In addition, the grating mount should be modified so that its adjustment screws can be turned by a ball-end wrench through holes in the temperature-control enclosure of the assembled laser. A good way to do this is to remove the heads from 1/4 in.-20 socket screws in a lathe and to attach them to the centers of the knobs of the adjustment screws with epoxy cement.

E. Piezoelectric disks

Piezoelectric (PZT) disks are inserted between the grating mount adjustment screw and the movable face of the mount in order to rotate the grating about a vertical axis and alter the cavity length with electrical control (Fig. 6). Each PZT element consists of a thin brass backing about 1 in. in diameter to which a thin smaller-diameter silver-plated piezoelectric slice is attached in the center with adhesive around its edge. When voltage is applied, the piezoelectric stress causes the backing to "dish" on the opposite side. Two such elements can be attached back to back, doubling the displacement of a single one, by lightly soldering the adjacent brass backings at four places around their circumference. If necessary for clearance in the grating mount, some of the excess brass can be clipped away without damaging the piezoelectric center. The double PZT is wired by lightly soldering one connection to the brass and the other to the two silver-plated piezo elements in parallel. For this and all other wiring of the laser, it is best to select a limp insulated wire that will not transmit vibration to the laser structure. Rubber covered No. 24 test prod wire has been found suitable. After the PZT is assembled and wired, and the grating is glued to the mount, the PZT should be inserted between the mounting plate and the ball end of the adjusting screw as shown in Fig. 6. Small pieces of mylar should be inserted to electrically isolate the PZT from the mount. The PZT will provide about ± 1 μm of displacement when ± 15 V are applied.

F. Enclosure for the laser

An aluminum enclosure should be fabricated to hold the laser. It should have a sufficient thermal mass and conductivity to aid in temperature stabilization. Such a box can be made out of rectangular side plates screwed together, placed on a rectangular baseplate, and capped by a lid, or a single piece of hollow rectangular tubing may be selected to form the walls. Wall thickness should be 1/4 to 1/2 in. Inside dimensions about 3.5 in. wide, 5.5 in. long and 4 in. high are adequate. The floor of the enclosure should stand on some firm support, to bring the laser output beam to a desired height above the table. The lid of the enclosure should be easily removable to allow frequent access to the laser with minimal disruption of the thermal or mechanical stability. After the laser is assembled and satisfactorily aligned, drill holes in the box to allow access to the grating adjustment screws and drill an opening to allow exit of the laser beam. These steps should be delayed until one knows for certain where the holes should be placed. The output aperture is ultimately covered by a microscope slide, and the access holes should be plugged to limit air currents.

Tapped holes on opposite edges of the bottom plate of the enclosure allow the laser structure to be anchored onto the vibration isolation pads discussed below, for instance by stretching a rubber band over the laser baseplate and looping it over screw heads in the edges of bottom plate.

The bottom edge of one of the side walls of the enclosure should be provided with a notch or channel at both ends of the laser for egress of all wires. Soft rubber placed in the notches can serve to press the wires firmly against the bottom plate, and in this way the movement of wires outside the box will not transmit stress or vibration to the laser structure. Finally, one should make sure the enclosure is electrically grounded.

IV. TEMPERATURE CONTROL

Precise control of the temperature of both the baseplate and the diode laser itself is essential for the long term reliable operation of the laser at a particular wavelength. We control these temperatures using identical independent servosystems. The sensing element for the servo is a small thermistor, which is part of a bridge circuit. The amplified and filtered error signal drives a heater or thermoelectric cooler. In this area of thermal control we have made the largest compromises of potential performance in order to simplify the mechanical and electrical designs. Part of the reason we are willing to make this compromise is that we usually sense the output frequency of the laser and lock it directly to atomic transitions to insure long term stability at the sub-MHz level. This is discussed in Sec. X.

The temperature of the diode laser mounting block is controlled only by heating, which means that it must be kept 1–2 °C hotter than the baseplate for proper temperature control. The heating is done by a small (0.3×1.5 in.) adhesive film heater which is attached to the top or side of the laser mounting block. The sensing thermistor rests in a small hole packed with heat sink compound in the mount-

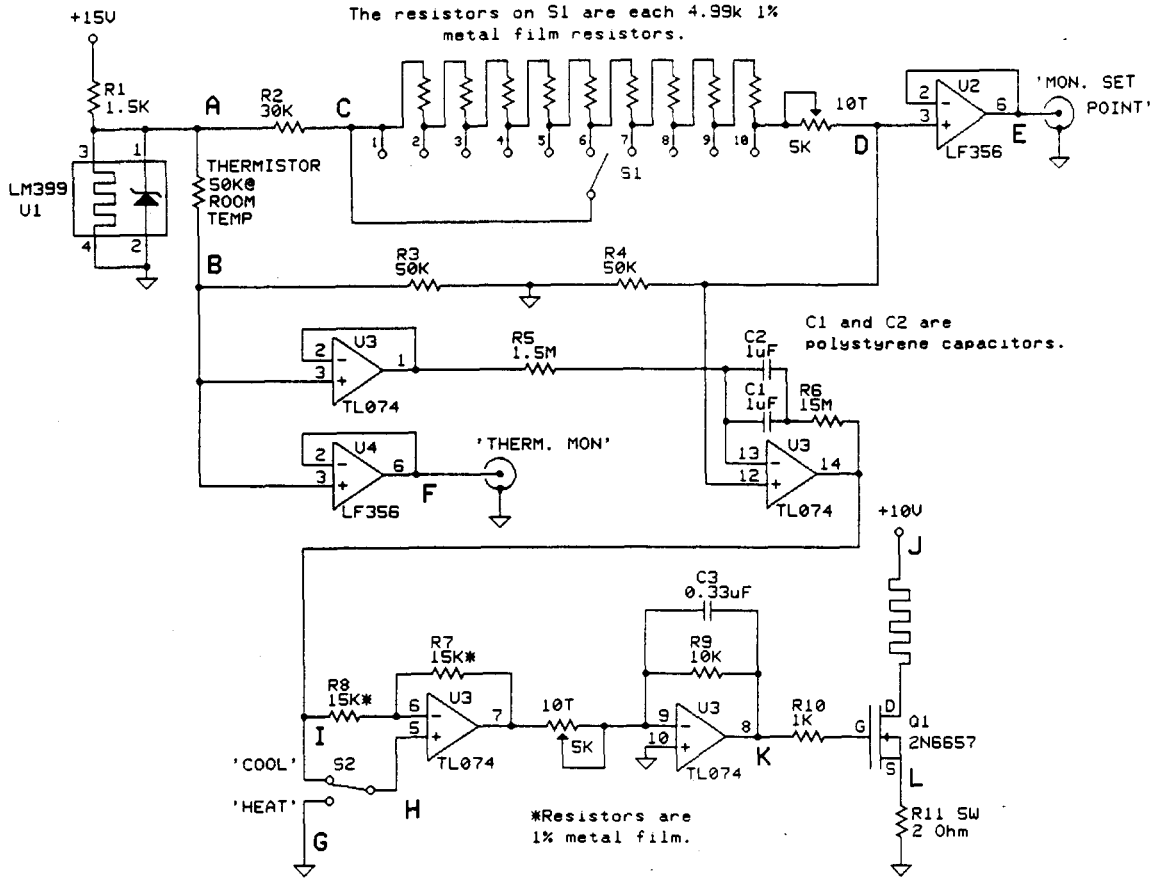

Fig. 7. Temperature control circuit.

ing block. The temperature control circuit which drives the heater is shown in Fig. 7. Although this circuit is rather crude compared to what is usually used for precision temperature control, we have found it adequate for most purposes. It is simply a bridge, an amplifier and an RC filter which rolls off the gain as 1/frequency, for frequencies between 0.005 and 0.50 Hz. The components have been chosen so that above 0.5 Hz the electrical gain is constant. This frequency response was selected so that the combination of this electrical response and the thermal response of the laser mounting block results in a net servo gain which goes nearly as $1/f$. The gain is set by the 5-kΩ potentiometer to be just below the point where the servo loop oscillates.

One can readily observe saturated absorption spectra and carry out other atomic spectroscopy experiments with temperature control only on the laser mounting block. However, temperature stabilizing the baseplate greatly reduces the thermal drift of the laser frequency and changes in the cavity alignment. The baseplate is either heated or cooled depending on the requirement. Heating is much simpler since it only requires the attaching of a film heater to the baseplate. The film heater is similar to that used on the laser, except it is larger in area and power output. To keep the baseplate controlled it is necessary that it be at least 1–2 °C above the room temperature, and the laser must be an equal amount hotter than the baseplate. This is not difficult if the laser's free running wavelength at room temperature is shorter than wavelength desired. In that case it is advantageous to heat the laser. If however the laser's free-running wavelength is significantly to the red, the laser should be run near or below room temperature. In this case, the baseplate must be cooled below room temperature using a thermoelectric cooler (TEC). This is somewhat more trouble, and the vibration isolation pads between the baseplate and the bottom of the enclosure are now replaced by a rigid TEC. The TEC is a square 1.5 in. on a side and fits between the baseplate and the aluminum plate which is the bottom of the enclosure. A thin layer of heat sink compound is applied on both sides of the TEC to insure good thermal contact. The bottom plate of the enclosure must have a large enough surface area or be in contact with a thermal reservoir so that it does not heat up enough to cause "thermal runaway" of the TEC. The baseplate temperature is monitored using a thermistor glued onto the middle of the baseplate. Since the thermal time constant for the baseplate is much longer, some adjustment (or removal) of capacitors $C1$, $C2$, and $C3$ from the temperature control circuit may be desirable to improve stability. If the laser is cooled below the dew point condensation may form. This may be avoided by flushing gently with dry N_2.

An alternative to controlling the baseplate temperature is to control the temperature of the entire enclosure. This is more effort because much more heating or cooling power is needed and the thermal time constant is very long. We find, however, that this technique gives better ultimate stability of the laser alignment. For most purposes, we have found that this is not worth the effort. However, the small additional effort required in putting insulation on the outside of the aluminum enclosure to attenuate room temperature fluctuations is worthwhile.

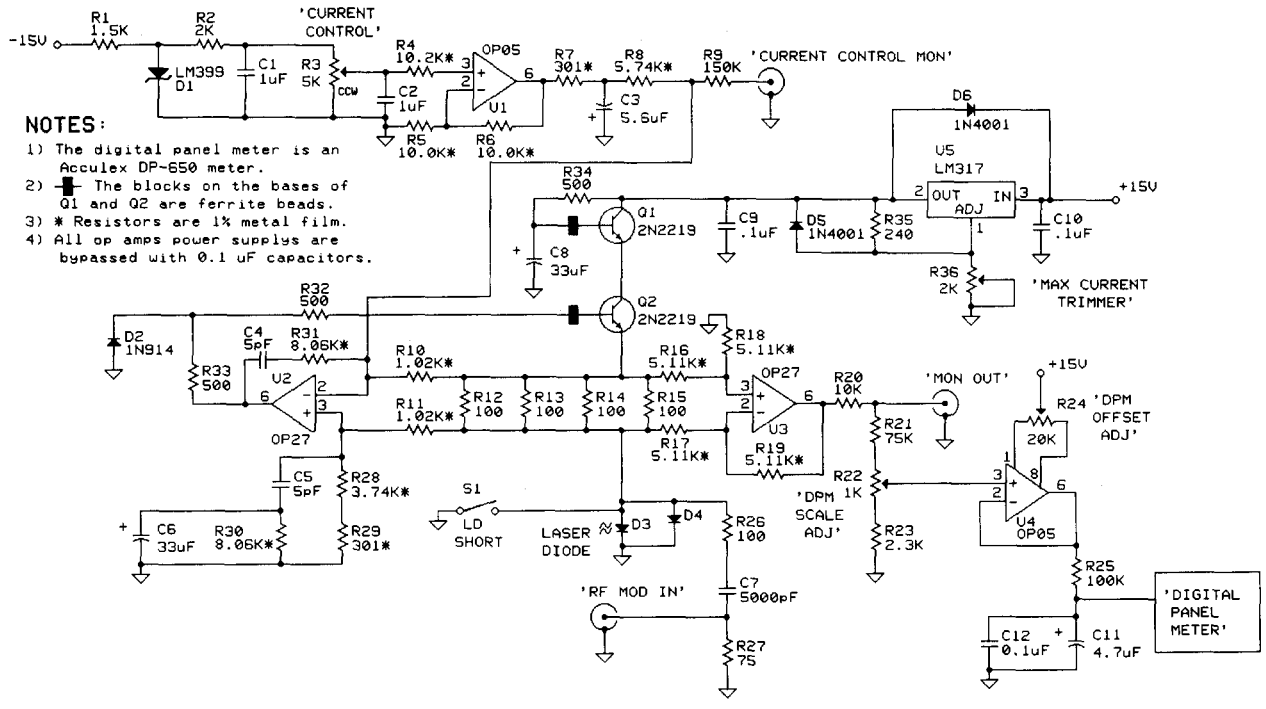

Fig. 8. Laser current control circuit.

V. LASER DRIVE ELECTRONICS

The circuit diagram[8] for the laser current controller is shown in Fig. 8. This is a stable low-noise current source. The output current can be modulated rapidly by sending a voltage into the "RF MOD IN" input. If such modulation is not needed and novices may be operating the laser, it is wise to disconnect or cover this input to minimize the possibility of accidentally damaging the laser. The output current of the supply is limited by potentiometer $R36$ to a value that cannot exceed the maximum allowed for the diode laser.

The primary concern when working with the current source is to avoid damaging the laser with an unwanted current or voltage spike. In Ref. 1, we discuss this danger at some length so here we will just provide a few helpful techniques. To avoid accidents we always carefully test a new power supply with resistors and light emitting diodes in place of the laser. We check that it produces the voltage and current desired, and that there are no significant transients when turning it on or off. It is also wise to check that all the appropriate grounding connections have been made so that turning on and off nearby electrical equipment or static discharges do not cause current or voltage spikes that exceed the maximum allowed by the laser diodes. When making these tests it is important to realize that lasers can be destroyed by spikes that last only a fraction of a microsecond. Only after the power supply has passed all these tests is it connected to the laser. The cables from the power supply to the laser should be shielded and there should be no possibility of them being accidentally disconnected.

One has to be fairly careful in handling the lasers to avoid static discharges, and it is a good idea to keep the leads shorted together as much as possible. Normally such lasers come with handling instructions that should be followed. These instructions will usually also mention that a fast, reverse-biased protection diode should be connected across the laser leads at the laser mounting block. This diode protects against voltages spikes which may exceed the few volts of back bias a diode laser can tolerate. We have found that the lifetime of diode lasers is substantially increased by also connecting several forward-biased diodes across the leads at the same point as shown in Fig. 9. These diodes have a large enough voltage drop that current does not flow through them under normal operation. However, if there is a large forward voltage, these diodes turn on allowing the current to flow through them instead of the laser diode. It may also be helpful to place a 10-Ω current limiting resistor in series with the supply right at the laser diode (at LD+ in Fig. 9) and, if modulation much above 1 MHz is not required, ferrite beats on the supply lead at this point. Switch $S1$ in Fig. 8 should be used to short the

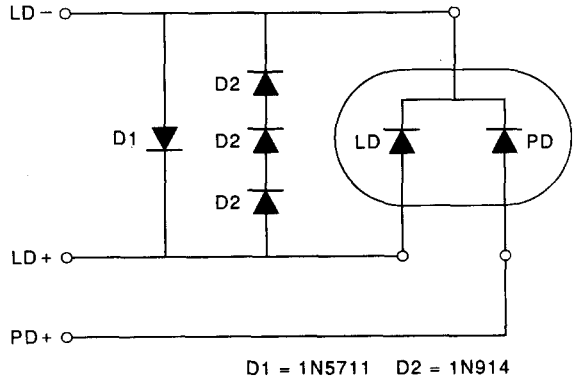

Fig. 9. Protection diode wiring to laser.

supply to ground before connecting the laser, and the current control $R3$ should be fully "off" whenever $S1$ is toggled.

VI. ASSEMBLY AND TESTING

A top view of the assembled laser is shown in Fig. 1.

A. Diode mounting

The laser diode, with its protection diodes already wired on and its leads temporarily shorted together for safe handling, is mounted in its recess in the laser mounting block with the screws only gently tightened at first. The desired orientation of the laser will produce a vertically polarized output beam and a widely diverging elliptical beam pattern whose major axis is horizontal. This corresponds to the rectangular output facet of the diode chip having its longer dimension vertical.

Next, the mounting block is attached to the baseplate by 4-40 screws extending from beneath. The baseplate should then be secured to some temporary stand so that the uncollimated laser beam can be easily observed after it has gone 1.5 m or more from the laser. The current supply is then set to a normal operating current. The output beam at 780 nm, when projected onto white paper attached to the wall, will hardly be visible with the naked eye, but will show up readily in an IR viewer. The 852-nm light can only be observed by the viewer or an IR sensitive card. At this time, interference rings or fringes may be apparent in the projected beam. These are normally caused by dust, fingerprints, etc., on the laser's output window. The window should be cleaned with an optical tissue dampened in methanol so that the beam pattern is uniform and clear. The orientation of the diode in its recess should be set either by noting the major axis direction or by checking the output polarization. Once the proper orientation is achieved, the mounting screws that hold the laser in its recess should be tightened. Make sure that connections to the diode, including the network of protection diodes, are insulated and arranged so that short circuits will not occur during routine handling. Note carefully the center position of the dispersed beam spot, both its height and lateral position and mark it on the wall. Despite the broad and undifferentiated beam spot, the center can be judged reliably within $\pm 2°$.

B. Collimation

The next step is collimation of the output beam and shimming, if necessary, of the laser or lens mounting blocks to the correct height. The collimating lens should be firmly fastened into its mounting block with a set screw and the mounting block should be loosely screwed to the laser baseplate with the flat side of the lens toward the diode. The precision adjusting screw that pushes against the baseplate hinge should be advanced so that the hinge is opened enough to allow plus and minus 0.020 in. of motion without losing contact with the ball end of the screw. Next insert a clean microscope slide (about 1-mm thickness) between the lens flange and the front face of the diode laser mounting block. While holding the lens block, the slide, and the diode block together with finger pressure, observe the beam spot again with the IR viewer. It should be possible to slide the lens block back and forth to bring a more concentrated intensity maximum near to the original aiming point of the laser. Temporarily tighten the screws that hold the lens block in that position and remove the slide. Next, adjust the precision screw to bring the laser beam to a sharp focus on the wall. By a very slight adjustment of the screw the beam should then be brought to collimation in an oblong spot about 5 mm wide. It should be confirmed that no focus occurs between the laser and the wall. This constitutes a preliminary alignment.

The beam spot will very likely fall 2° or more from the aiming spot. Horizontal corrections can be made smoothly by use of the alignment jig later, but vertical corrections require shimming first. Note the vertical displacement of the spot from the aiming point. A low spot will require raising the lens mount by about 0.0025 in. per degree of misalignment and a high spot will require raising the diode block by the same amount. Layers of aluminum foil (avoiding crinkles) or shim stock should be selected to shim the preliminary alignment beam height to within 1° of the aiming spot.

The alignment jig is installed next by screwing it to the laser baseplate using its oversize hole and a large washer (or stack of washers) so that it snugly touches the lens mount as shown in Fig. 4. It should be positioned with its 2-64 screw and a spring or elastic cushion so that when the screws of the lens mount are released, the mount can be pushed in both directions without losing contact. With the lens-mount screws now loosened the mount may be displaced smoothly to bring the collimated spot horizontally to the aiming point. A rubber band or finger pressure should be used to hold the loose lens mount against the jig.

A properly aligned laser will exhibit a symmetrical and elliptical beam spot. The effects of aberration can be observed by purposely misaligning the lens to one side or the other with the jig, and a symmetrical behavior allows one to confirm that the designated aiming spot was initially correct. After a satisfactory alignment and collimation has been obtained, the lens mount screws should be firmly tightened and the jig removed. After the lens mount is tightened in place, the fine adjustment screw should again be adjusted to precisely collimate the beam. Positioning the lens without the jig is also possible for those users with a steady hand, but it is very difficult to avoid random rotations and displacement along the beam when only a transverse adjustment is desired.

C. Power output and threshold current measurements

After the laser has been aligned and collimated and before the grating is installed, the power output and threshold characteristics should be recorded and compared with the specifications. The threshold current depends on laser temperature, so it may be desirable to stabilize the temperature of the diode mount at this time. The output power can be measured as a function of drive current by illuminating the face of a wide-aperture photodiode.

D. Mounting and adjusting the diffraction grating

The mounting of the diffraction grating has been described earlier. The laser cavity length is determined by the distance from the back of the laser chip to the illuminated spot on the grating and can be as short as about 20 mm in this design. The grating mount should be screwed to the laser baseplate to form a cavity of the desired length so that the collimated beam illuminates the center of the grating at

approximately the Littrow angle. Best results have been obtained with the shortest possible cavities, apparently because the corresponding mode spacing (about 8 GHz) avoids excitation of adjacent cavity modes by the inherent relaxation noise of the diode at around 3 GHz from line center. It is possible, with a carefully aligned 780-nm laser having 20-mm cavity length to tune electrically over 7 GHz without a mode hop using only the PZT.

The following procedure is used to align the diffraction grating. A small card cut from stiff white paper or a file folder, about $2\times 1/4$ in., is useful as a probe to see that the beam diffracted from the grating returns approximately to the center of the lens. The beam spot at 780 nm is readily visible to the eye on the card, but at 852 nm the IR viewer is required. Before screwing the grating mount firmly to the baseplate in this coarse alignment make sure that the adjustment screws are in midrange. The card should be used next to make a more careful alignment of the grating. If the return beam is, for example, too high, as the card is lowered vertically in front of the lens the outward face of the card will be illuminated along a narrow region at its edge until the beam is completely cut off. The width of this narrow region indicates the degree of vertical misalignment. When an edge of the card is raised from below to cut off the beam, no such region of direct illumination will be visible in this example, although direct light from the lens may weakly filter through the card. Probing from all four directions into the collimated beam will indicate both the horizontal and vertical misalignment of the return beam, and the objective is to adjust the screws of the grating mount so that the width of the illuminated region on the card edge is brought exactly to zero for each direction of approach.

A precise vertical alignment of the return beam is made by reducing diode current to just above threshold. Then observe the intensity of the output beam while adjusting the tilt of the grating around a horizontal axis. If the preliminary Littrow alignment was adequate, the output beam should significantly brighten at the exact vertical position that optimizes feedback into the diode. After completing this adjustment the threshold current will be lower than the value recorded earlier for the diode. The laser should now be operating with grating controlled feedback near its free-running wavelength.

If more than one vertical setting of the grating appears to enhance the laser output near threshold, or if the output beam projected on a distant surface consists of more than a single collimated spot, the fault may lie with imperfections (chips, scratches, dirt) on the grating, laser window, or lens surfaces.

VII. TUNING THE LASER FREQUENCY

A low-resolution ($\leqslant 1$ nm) grating spectrometer is useful to assess the tuning characteristics of the laser discussed below. After initial alignment of the grating, the output wavelength of the laser will be within about 2 nm of the wavelength specified by the manufacturer, and near the center of the tuning range. Small adjustments of the grating rotation screw (vertical axis) should smoothly shift the laser wavelength. A region of the grating angle adjustment should be identified over which the laser can be tuned. As one nears the end of the tuning range the laser output will be seen to hop back and forth or share power between two very different frequencies. One is the fixed "free-running" frequency at which the laser will operate if there is too little or no feedback from the grating, and the other is the angle dependent frequency set by the grating feedback. At a given temperature, tilting the grating should tune the output wavelength over a range 10 to 30 nm, depending on the particular laser and the amount of feedback. Changing the diode temperature shifts the entire range by 0.25 nm/°C. If the grating is misaligned, the output wavelength will either be insensitive to small changes of the grating angle or will move only a small amount and then jump backwards.

Although this tuning may appear continuous when observed on a low or medium resolution spectrometer, there can actually be small gaps. These occur because the wavelength-dependent feedback of the grating dominates but does not always totally overwhelm feedback off the AR coated output facet of the chip. If it proves impossible to excite some desired atomic absorption line by tilting the grating, it is necessary to operate at a different temperature and/or current. This is best assessed by means of an atomic absorption cell (discussed below) since the gaps in tuning can be narrow and vary randomly from one laser to another. It is helpful to record the tuning rate vs grating rotation (about 14 nm/turn with an 80 thread-per-in. screw pitch), because one can easily mistune the grating grossly, requiring a retreat to earlier steps in the alignment process. After the grating rotation has been set to produce approximately the correct wavelength, the vertical alignment should be rechecked using the threshold current technique.

The simple laser design described here suffers from a defect that may be annoying in wideband usage: Its output beam is deflected horizontally as the wavelength is scanned, approximately at the angular rate,

$$\frac{d\theta_{\mathrm{BEAM}}}{d\lambda}=[d^2-(\lambda/2)^2]^{1/2}\approx 0.08 \text{ deg/nm},$$

for grating constant d. This is normally of no consequence, however, for saturated absorption or neutral atom trapping, e.g., in Rb where the $5s_{1/2}-5p_{3/2}$ hyperfine multiplets of the two naturally occurring isotopes span a total of less than 0.014 nm. If it is necessary to avoid beam deflection, the simplest technique is to take the output beam off a beam splitter inserted between the collimating lens and the grating.[1]

VIII. ENCLOSURE AND VIBRATION ISOLATION

After all preceding steps of alignment have been completed, the laser should be thermally and vibrationally isolated in its enclosure. We have achieved an adequate degree of mechanical isolation by supporting the laser inside the enclosure on three rubber pads that form a tripod under the solid part of the baseplate (avoiding the hinge). Soft "sorbothane" rubber, 1/8 in. thick, cut into 1/2-in. squares and stacked to a height 3/8-in. forms a springy but well damped support that isolates from vibrations above about 100 Hz. For extra isolation, additional rubber may be placed under the support which holds the enclosure at the desired height. The wires from heaters, thermistors, the diode, and the PZT should be taped down to the laser and/or the enclosure baseplates to decouple them mechanically from the laser cavity. The suggested enclosure design offers additional decoupling by pressing the wires firmly against the bottom plate where they exit from the box.

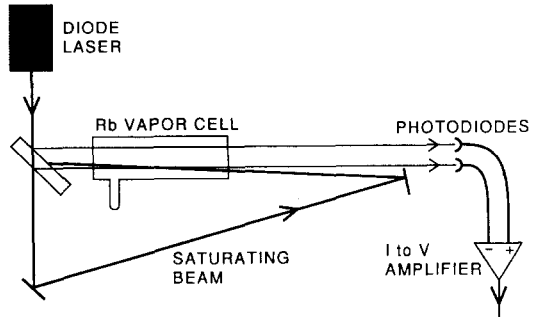

Fig. 10. Beam layout for saturated absorption.

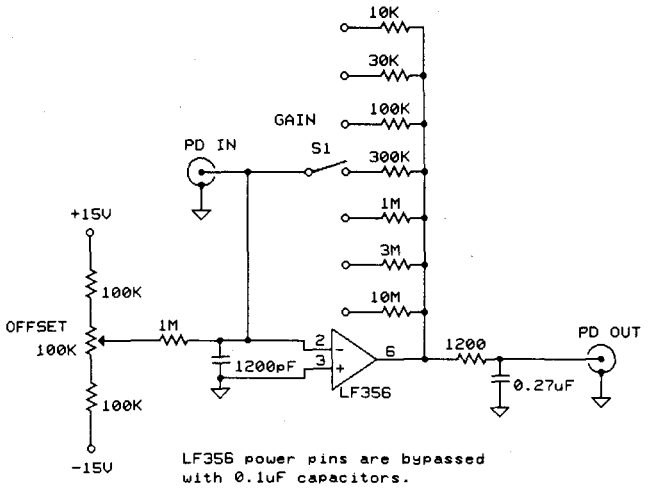

Fig. 11. I to V amplifier circuit.

Holes should now be drilled in the sidewalls of the box to allow the beam to exit and to allow manual grating adjustments without having to open the enclosure. Because of the very nonrigid support of the laser, mechanical adjustments, although not often necessary after stabilization, require a delicate touch. The laser structure takes one or more hours to fully stabilize inside its box with temperature-control electronics active. However, preliminary output tests can proceed immediately if steady frequency drift is not an obstacle.

Depending on the degree of stability required and the environment, the laser may be operated on anything from an ordinary laboratory bench, to a fully isolated optical table. A room location near a load-bearing wall or in a basement laboratory can often be worth the price of an expensive optical table. Since the laser itself is one of the best vibration detectors obtainable, experience will be the best guide.

IX. SATURATED ABSORPTION SPECTROMETER

The simplest spectroscopy one can perform with these lasers is to observe the absorption and Doppler-free saturated absorption spectra[9] of rubidium or cesium. This can easily be done in small glass vapor cells which are at room temperature. Such spectroscopy experiments also provide the simplest way to determine the short and long term frequency stability and tuning behavior of the laser frequency.

A. Vapor cells

Rubidium and cesium vapor cells can be obtained commercially, but they are usually rather expensive. However, they can be prepared quite easily, if one has a vacuum pump and some basic glassblowing skills. We use pyrex or quartz tubing, typically 1 in. in diameter and 2 to 4 in. long, and fuse windows onto the ends. The optical quality of the windows is unimportant. The glass cell is connected to a vacuum system through a glass tube about 1/4-in. diameter so that the cell can be evacuated to between 10^{-5} and 10^{-6} Torr. After the cell is filled, it will be "tipped off" by heating this connecting tube until it collapses in on itself. A few grams of alkali metal in a glass ampule are placed in a separate arm on the vacuum system. The system should be pumped down and the cell outgassed briefly by heating it for several minutes with a torch. At the point where it will be tipped off, the glass connecting arm should be repeatedly heated until it just starts to soften but does not collapse in. After the outgassing is completed, the ampule should be broken to release the alkali metal into the system. Often when one purchases ampules of alkali metal they come packed with an inert gas. In this case there will be a burst of gas also released into the system which must be pumped away. The alkali metal can be moved into the cell simply by heating the glass around it and thus distilling it down the glass tubing into the cell. It is only necessary to have a few very small droplets in the cell so one ampule is sufficient to fill many cells. It is desirable to put much less than 1 g of metal into the cell to reduce the tendency of the metal to coat the windows. Once the alkali is in the cell, the sidearm is tipped off and the cell is ready for use.

B. Optical setup

Figure 10 illustrates a typical layout of beams for a simple saturated absorption apparatus. Initially only a single beam passing through the cell is required, which should be the full laser intensity for maximum sensitivity. In this step one tunes the laser to an atomic transition and finds the optimum laser temperature, current, and mechanical arrangement for stable operation. When the cell is viewed through an IR viewer, or a CCD television camera, a strong track of fluorescence should become visible as the laser is tuned within the Doppler profile of an absorption line by mechanically rotating the grating. It is helpful to ramp the PZT at a frequency of 20 Hz over a 15-V range during this search. The diode current should be arbitrarily set between about 75% and 90% of I_{op}. If no fluorescence is apparent at any grating angle with the known tuning range, the temptation to turn the grating farther or to adjust the vertical alignment of the grating should be resisted. Most likely the laser has a tuning discontinuity that encompasses the desired wavelength. The current should be changed several mA and the procedure repeated. If this still fails, the temperature should be changed up or down 0.5 °C to 1 °C and the search for the absorption line should be repeated. If this process is iterated several times without success, it may be desirable to look once again with the grating spectrometer to confirm that the laser is still tuning in the desired range and that the grating has not been grossly misaligned by a random walk. When one finds a grating position which produces fluorescence, the current can be adjusted to maximize the fluorescence.

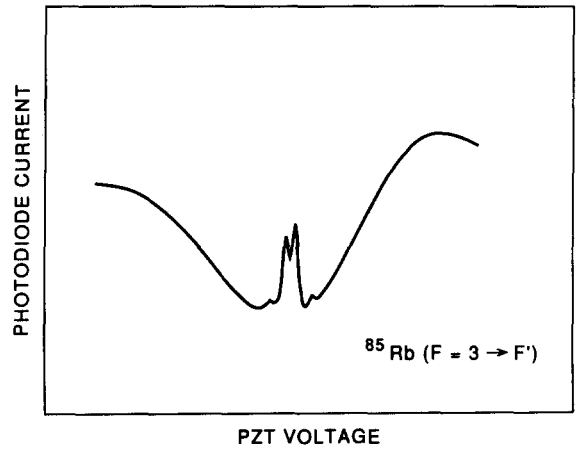

Fig. 12. Single beam saturated absorption in ^{85}Rb, $F=3\rightarrow F'$.

Once a proper temperature has been set it should not be necessary to change it. However, when the laser is turned on in the morning it is not uncommon to find that the proper drive current has changed by up to 1 mA, or, at a fixed current, minute readjustment of the grating angle is needed, to hit the absorption line again. This drift may be caused by environmental changes, hysteresis in the electrical tuning characteristics, aging of the diode, or mechanical creep of laser cavity components.

C. Piezoelectric scanning

After the laser is mechanically tuned onto an absorption line as observed in the IR viewer, the transmitted (probe) beam should be attenuated so that the intensity is less than 3 mW/cm^2 and directed into a photodiode. A preliminary assessment of mechanical, electrical, and thermal stability may be made merely by observing the single-beam absorption line. The photodiode output is converted to a voltage by an I/V amplifier, whose circuit is shown in Fig. 11, and the resulting signal is displayed on an oscilloscope. Make sure the I/V offset is not set to an extreme value that saturates the amplifier at either the positive or negative supply voltage. Next the piezoelectric element should be driven by a triangle wave from an ordinary function generator at 15 to 30 Hz, with peak-to-peak amplitude up to 30 V. The photodiode signal should vary by 5%–50% (depending on the particular cell) as the PZT scans the laser across the absorption line. It is helpful to trigger the scope from the function-generator sync pulse or TTL output, or operate the scope in X–Y mode in order to obtain a stable display as the PZT drive is adjusted. When electrical tuning of the laser over the absorption line has been obtained, it is a good time to reexplore mechanical adjustments of the grating angle and diode drive currents. An absorption line or its neighbors, corresponding to different hyperfine levels of the ground state or different isotopes, recurs several times for nearby currents or grating angles. Also discontinuous steps of photodiode output occur across the oscilloscope trace. These steps correspond to transitions from one longitudinal external cavity mode to another. These mode hops may be as far as 8 GHz apart but will exhibit somewhat random spacings as well as hysteresis.

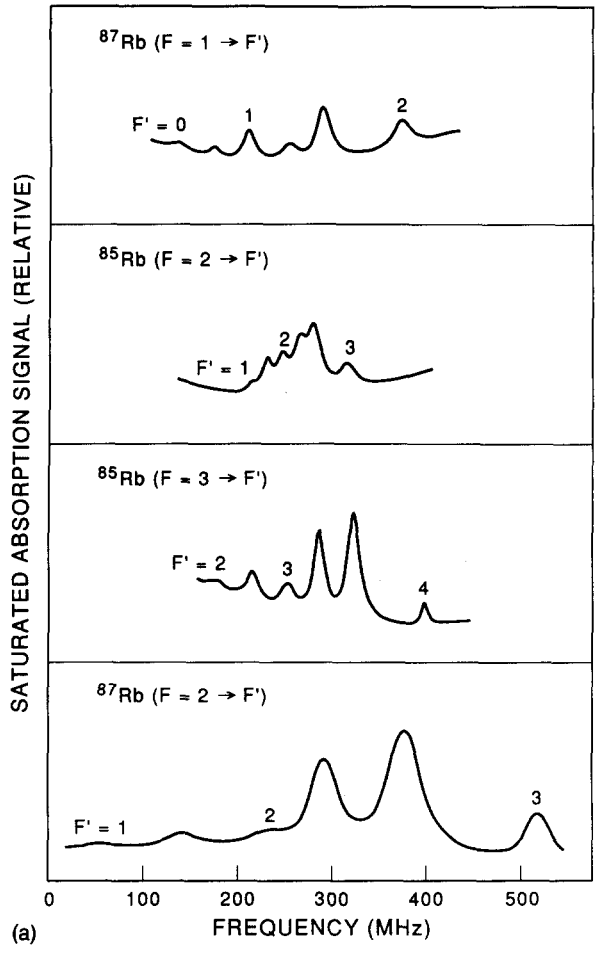

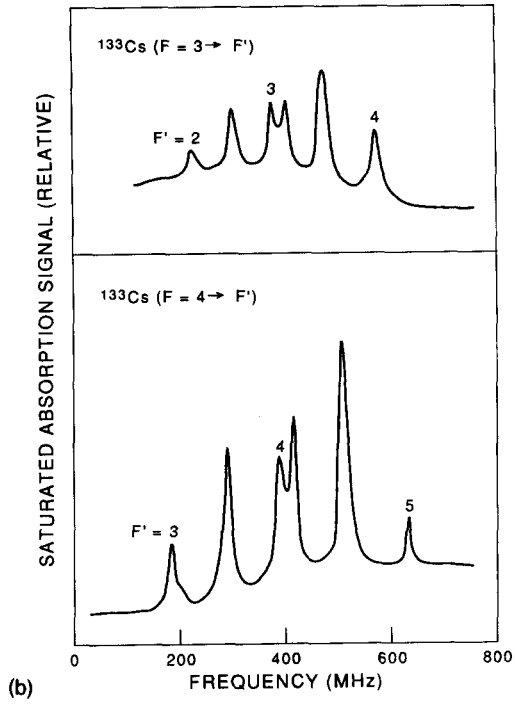

Fig. 13. Saturated absorption curves for (a) Rb and (b) Cs. The ^{87}Rb $F=2\rightarrow F'$ peaks are broader than the others because they were made with a different setup. The widths and relative heights are affected by beam alignment, beam intensities, electronic damping constants, and absorption cell pressure. These are only representative results.

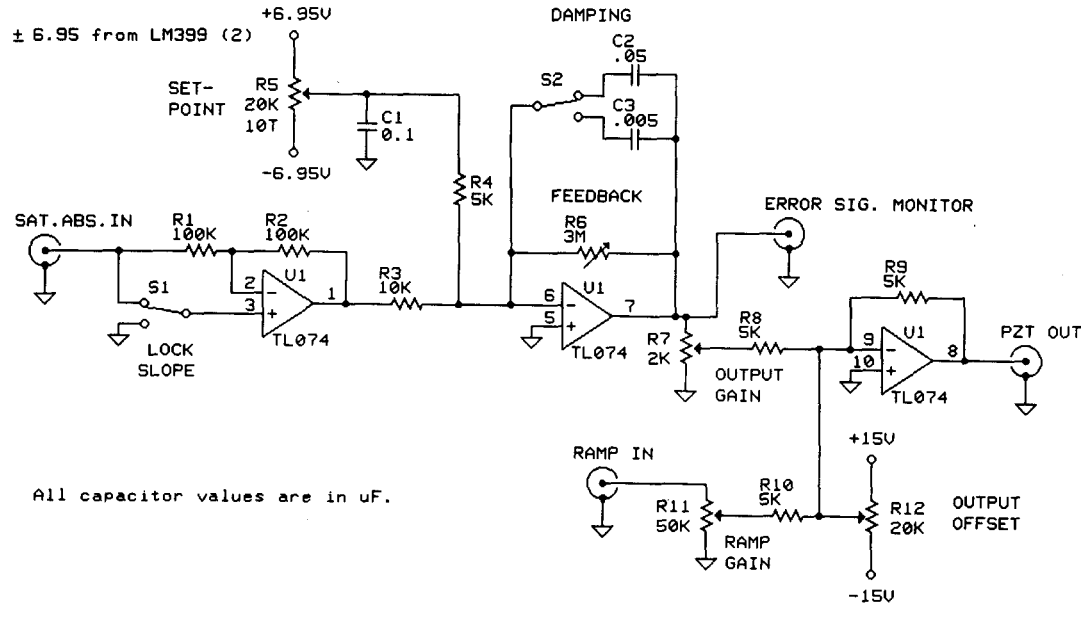

Fig. 14. Servolock circuit.

D. Observing the saturated absorption

The full saturated-absorption setup of Fig. 10 is required for a more detailed test of stability and tuning rates and for locking of the laser output frequency at the level of 1 MHz or better. When first observing a saturated absorption signal it is useful to block the nonoverlapped probe beam. The counter propagating saturating beam can easily be aligned to overlap the probe beam at a 1° intersection angle or smaller. The intensities of the beams are not important for initial adjustments, but typically only a small fraction of the laser output, less than a few percent should be used for the saturated absorption. Reflection from a microscope slide provides an ample intensity that will allow further attenuation by neutral density filters or exposed photographic film. When adequate pump and probe beam overlap has been obtained, small saturated absorption dips should become evident near the center of the absorption line (Fig. 12). They may be recognized unambiguously by their disappearance from the Doppler profile if the saturating beam is blocked. The height of the narrow dips may be maximized by adjusting the alignment. The width can be reduced by reducing the angle of intersection of the overlapped beams and by attenuating either or both beams to avoid power broadening. The triangle wave amplitude and dc offset can be adjusted to zoom in on a particular region of the scan.

For more detailed observations it is helpful to unblock the second probe beam. This second probe beam is directed into a photodiode identical to the first and wired in parallel with reversed polarity. The two probe beams can easily be obtained by utilizing the reflections off both front and rear surfaces of a piece of 3/8-in.-thick transparent plastic or glass. When the two photodiodes are properly positioned, the differential output signal cancels the large and featureless Doppler profile of the absorption line and allows saturated absorption features from the first probe beam to appear on a nearly flat background. If the Doppler broadened absorption is observed but the saturated absorption peaks cannot be seen, it often means that there is too much background gas in the vapor cell.

E. Saturated absorption patterns in Rb and Cs

After saturated absorption peaks have been observed, one can compare the patterns to known hyperfine structures of the ground and excited states to assess the electrical tuning range possible without hopping external cavity modes and to establish the tuning direction. The widths and resolution of the saturated absorption peaks for a given resonance line will depend on electronic time constants, the triangle-wave frequency, and possibly on diode current, in addition to alignment and intensity factors noted above. Figure 13 shows several saturated absorption patterns in Rb (780 nm) and Cs (852 nm) vapors photographed from an oscilloscope. These may aid new users in finding their way. Note that the patterns contain both true Doppler-free peaks and crossover peaks,[9] which occur at frequencies $(\nu_1+\nu_2)/2$ for each pair of true peaks at frequency ν_1 and ν_2. The crossovers are often more intense than the true peaks.

F. Typical tuning rates observed by saturated absorption

Tuning rates for the grating-feedback laser, operated with a single longitudinal mode of the external cavity, depend on geometrical, thermal, and electrical properties of the laser components. In particular, tilting the grating changes both the wavelength of light diffracted back to the diode and the length of the cavity. These two effects interact in determining the change of output frequency. Typical tuning rates for a 780-nm laser having a 20-mm cavity on an aluminum baseplate are: (1) diode drive current: 200 MHz/mA, (2) temperature change of diode: 4 GHz/°C, (3) temperature change of baseplate (cavity length): 7 GHz/°C, (4) grating angle change (80 pitch screw): 5 $\times 10^6$ MHz/turn, and (5) piezoelectric tuning: 1 GHz/V.

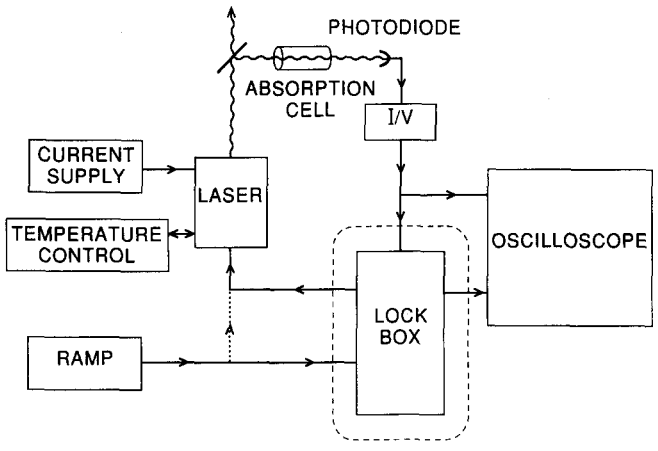

Fig. 15. Electronic layout schematic. For operation without the servolock box, the ramp is connected directly to the PZT as shown by the dashed line.

X. SERVOLOCKED OPERATION OF THE DIODE LASER

For stabilized operation of the laser, it may be locked to either side of any of the sufficiently well-resolved saturated absorption peaks such as those shown in Fig. 12. A simple servolock circuit is given in Fig. 14. Figure 15 indicates how the lock box is connected to the other components. Locking is not difficult after a little practice, provided that the saturated absorption signals are not too noisy and the laser frequency jitter caused by environmental or electrical backgrounds is less than the saturated absorption linewidths.

First, the laser is tuned to the desired hyperfine multiplet of saturated absorption peaks and the ramp gain and ramp offset are adjusted, both on the ramp generator and on the lock box, so that one can zoom in to the desired side of a particular peak simply by turning down the ramp gain on the lock box to zero. With feedback and output gain controls set at minimum and the laser tuned to the side of a peak, the error offset is adjusted to a value near 0 V, as observed on an oscilloscope. The feedback and output gains are then gradually increased until the circuit corrects for deviations from the desired lock point and thus holds the frequency on the side of the peak. If the servolock seems to "repel" the saturated absorption peak, the input invert switch is reversed to select the opposite slope. When the laser is properly locked, it should be possible to turn the feedback fully on and the output gain up to a point where the PZT begins to oscillate at about 1 kHz. The best operating point is just below the onset of oscillation. Locking is confirmed by noting that the setpoint, indicated by the level of the now flat saturated absorption signal on the oscilloscope, can be varied by the error offset control within a range from about 10% to 90% of the height of the selected peak without a noticeable change in the monitored error output. Independently, the error output can be varied over a wide range by the ramp offset control without affecting the locked level of the saturated absorption signal.

When the laser is locked, environmental noise appears on the error output and error signal monitor instead of on the saturated absorption signal because the error output compensates for laser frequency variations that would otherwise occur. The error signal monitor thus becomes an excellent indicator of the magnitude and spectral characteristics of the compensated noise, out to the bandwidth of the servolock circuit.

The drift rate of the unlocked laser is normally under 5 MHz/min when the system is properly stabilized, and this slow drift is eliminated by locking. The short-term jitter amplitude of the unlocked laser frequency is typically ± 3 MHz on a 1-s time scale if the laser is on a reasonably stable lab table. The short-term intensity variations are much smaller than 1%. When locked, the laser frequency is stabilized to 1 MHz or better.

The locked diode laser described in this paper is well suited for studies of neutral-atom cooling and trapping, for which some elaborations of the servolock circuitry are desirable. A future paper will describe trapping of Rb and Cs atoms from a vapor cell in a user-manual style similar to that used here.

ACKNOWLEDGMENTS

This work was supported by the NSF and ONR. We are indebted to many people who contributed ideas which have been incorporated into the present design. Much of the basic design work was carried out by Bill Swann, Kurt Gibble, and Pat Masterson. Steve Swartz, Jan Hall, and nearly every member of the Wieman group during the past several years have also provided valuable contributions. Melles Griot Inc. loaned us an excellent diode laser current supply which was used for part of this work.

APPENDIX: PARTS AND SUPPLIERS

1. Collimating lens #1403-.108, $75.00, $f=5$ mm, numerical aperture 0.5, Rodenstock Precision Optics Inc., 4845 Colt Road, Rockford, IL 61109, (815) 874-8300

2. Sorbothane Pad P/N: C37,000, $49.95, Edmund Scientific, 101 E. Gloucester Pike, Barrington, NJ 08007-1380, (609) 573-6250

3. Photodiode Pin-10D (1 cm^2 active area), $55.25, United Detector Technology—Sensors, 12525 Chadron Avenue, Hawthorne, CA 90250, (213) 978-1150 x360

4. Kodak IR detection card R11-236, $49.50, Edmund Scientific, (address as above)

5. Hand held infrared viewer P/N 84499, $1195.00, FJW Optical Systems, Inc., 629 S. Vermont Street, Palatine, IL 60067-6949, (708) 358-2500

A less expensive alternative is to use a CCD surveillance camera. These can be purchased from many sources including home and office security companies, and discount department stores. For an adequate model, prices for a camera, lens, and monitor will range from $500 to over $1000.

6. Sharp Diode Laser LT025MDO, $170.85, wavelength 780 nm, Added Value Electronic Distributors, Inc. (local Sharp distributor), 4090 Youngfield Street, Wheatridge, CO 80033, (303) 422-1701

STC LT50A-034 laser diodes (STC was recently purchased by Northern Telecom), wavelength 852 nm. We have purchased these lasers for $\approx$$650 from a German distributor: Laser 200 GMBH, Argelsrieder Feld 14, D-8031 Werling, Germany

7. Minco Thermofoil Kapton Heater, Minco 8941 P/N HK5207R12.5L12A, $23.50, #10 PSA (Pressure sensitive

adhesive) sheet, $4.00, Minco Products, Inc., 7300 Commerce Lane, Minneapolis, MN 55432, (612) 571-3121 x3177

8. Diffraction grating 1200 1/mm, 500 nm blaze: P/N C43,005, $72.85, 750 nm blaze: P/N C43,210, $72.85, Edmund Scientific (address as above)

9. Thermistor, P/N 121-503JAJ-Q01, $8.25, Fenwall Electronics, 450 Fortune Blvd., Milford, MA 01757 (also available from electronics distributors)

10. PZT disk, P/N PE-8, $0.75 (Murata/Erie # 7BB-27-4), All Electronics Corp., P.O. Box 567, Van Nuys, CA 91408, (818) 904-0524

11. Kinematic Mirror Mount Mod. MML, $52.00, Thorlabs, Inc., P.O. Box 366, Newton, NJ 07860, (201) 579-7227

12. Fine Adjustment Screw Mod., AJS-0.5, $30.00, Newport Corp., P.O. Box 8020, 18235 Mt. Baldy Circle, Fountain Valley, CA 92728-8020, (714) 963-9811

13. Thermoelectric cooler, 30×30 mm, #CP1.4-71-045L, $19.00, MELCOR, 990 Spruce St., Trenton, NJ 08648, (609) 393-4178

14. Cesium and rubidium vapor cells. We have never used these cells, but this company has announced that they will sell low cost vapor cells to educational institutions. Environmental Optical Sensors, Inc., 3704 N. 26th St., Boulder, CO 80302, (303) 440-7786

[a]JILA Visiting Fellow 1991–1992. Permanent address: Department of Physics and Astronomy, University of Kentucky, Lexington, KY 40506-0055.

[1]C. Wieman and L. Hollberg, "Using diode lasers for atomic physics," Rev. Sci. Inst. **62**, 1–20 (1991).

[2]J. C. Camparo, "The diode laser in atomic physics," Phys. **26**, 443–477 (1985).

[3]R. Ludeke and E. P. Harris, "Tunable GaAs laser in an external dispersive cavity," Appl. Phys. Lett. **20**, 499–500 (1972).

[4]M. W. Fleming and A. Mooradian, "Spectral characteristics of external-cavity controlled semiconductor lasers," IEEE J. Quantum Electron. **QE-17**, 44–59 (1981).

[5]Diode lasers that are supplied without an output window, or diodes whose hermetic package has been carefully opened, may be AR coated with SiO by the user who has suitable optical coating apparatus, and improved operation may result. See M. G. Boshier, D. Berkeland, E. A. Hinds, and V. Sandoghdar, "External-cavity frequency-stabilization of visible and infrared semiconductor lasers for high resolution spectroscopy," Opt. Commun. **85**, 355–359 (1991).

[6]The user should be aware in evaluating gratings for use that the efficiency is highly sensitive to polarization. See E. G. Loewen, M. Nevière, and D. Maystre, "Grating efficiency theory as it applies to blazed and holographic gratings," Appl. Opt. **16**, 2711–2721 (1977).

[7]Steve Chu, Stanford Univ., private communication.

[8]Steve Swartz, Univ. of Colorado, private communication.

[9]For a discussion of saturated absorption spectroscopy, see W. Demtroder, *Laser Spectroscopy* (Springer-Verlag, New York, 1981).

Railgun recoil, ampere tension, and the laws of electrodynamics

A. E. Robson and J. D. Sethian
Plasma Physics Division, Naval Research Laboratory, Washington DC 20375-5000

(Received 16 December 1991; accepted 2 May 1992)

There has recently been a revival of an old controversy over whether Ampere's original law of force between current elements is to be preferred over the more familiar and universally used Biot–Savart–Lorentz law. Although it is agreed that the two laws give identical results when used to calculate the force between two circuits, it has been claimed that if Ampere's law is applied to the action of a circuit upon part of itself it predicts internal longitudinal forces that are excluded by Biot–Savart–Lorentz. The existence of longitudinal forces has been inferred from observations of the buckling of the rails in a railgun, attributed to compressive stress, and the fracture of long wires subjected to pulsed currents, attributed to "Ampere tension." An experiment has been performed that should provide an unambiguous demonstration of this longitudinal force, if it exists. The apparatus consisted of a rigid coaxial circuit in which an unsymmetrical section of the center conductor was free to move in the axial direction under the influence of the longitudinal force. Pulsed currents of up to 100 kA were passed through the circuit but no evidence of a longitudinal force was found. It is shown that this result is consistent with Ampere's force law, and that claims that the law predicts longitudinal forces are based on the incomplete application of the law.

I. INTRODUCTION

The original law of force between electric circuits was formulated by Ampere[1] who considered individual current elements to act upon each other as if they were Newtonian particles. He derived an empirical relationship for the force between current elements which, expressed vectorially, is

$$d^2\mathbf{F}_2 = -i_1 i_2 [2(\mathbf{ds}_1 \cdot \mathbf{ds}_2) - 3(\mathbf{ds}_1 \cdot \mathbf{r}_{12}) \times (\mathbf{ds}_2 \cdot \mathbf{r}_{12})/r_{12}^2]\mathbf{r}_{12}/r_{12}^3, \quad (1)$$

APPARATUS AND DEMONSTRATION NOTES

The downloaded PDF for any Note in this section contains all the Notes in this section.

Frank L. H. Wolfs, *Editor*

Department of Physics and Astronomy, University of Rochester, Rochester, New York 14627

This department welcomes brief communications reporting new demonstrations, laboratory equipment, techniques, or materials of interest to teachers of physics. Notes on new applications of older apparatus, measurements supplementing data supplied by manufacturers, information which, while not new, is not generally known, procurement information, and news about apparatus under development may be suitable for publication in this section. Neither the *American Journal of Physics* nor the Editors assume responsibility for the correctness of the information presented.

Manuscripts should be submitted using the web-based system that can be accessed via the *American Journal of Physics* home page, http://ajp.dickinson.edu and will be forwarded to the ADN editor for consideration.

An undergraduate measurement of radiative broadening in atomic vapor

A. J. Hachtel, J. D. Kleykamp, D. G. Kane, M. D. Marshall, B. W. Worth, J. T. Barkeloo, J. C. B. Kangara, J. C. Camenisch, M. C. Gillette, and S. Bali[a)]

Department of Physics, Miami University, Oxford, Ohio 45056-1866

(Received 9 April 2011; accepted 27 February 2012)

We show that one may quantitatively investigate radiative broadening of atomic transitions in the undergraduate laboratory using a traditional saturated absorption spectroscopy setup.

[http://dx.doi.org/10.1119/1.3694241]

I. INTRODUCTION

Optical spectroscopy of atomic fine structure and the Zeeman effect form an indispensable component of the modern undergraduate laboratory curriculum.[1] With the growing popularity of home-built tunable diode laser systems,[2] a demonstration of the hyperfine structure of alkali atoms using saturated absorption spectroscopy (SAS) (Ref. 3) is becoming an important experiment in many undergraduate optics laboratories.[4–6] A natural extension of SAS, which has not been traditionally emphasized, is to adjust the power of the pump beam and study the dependence of the hyperfine spectral linewidth on intensity. The purpose of this short note is to point out that one may use the SAS setup for an instructive investigation of radiative broadening, also known as power broadening, in room temperature atomic vapor.

Radiative broadening is an important fundamental phenomenon in light-matter interaction, attractive to students at many levels. Freshmen and sophomores are intrigued by the concept that the act of observing a spectral absorption line in an optical measurement broadens the linewidth. More advanced students are fascinated by the idea that even after various line-broadening mechanisms, such as Doppler broadening and pressure broadening, are suppressed, there still remain radiative broadening effects that prevent the observation of a spectral line with its "natural" linewidth, despite using low light-levels for the measurements. Radiative broadening of the spectral absorption profile occurs because the on-resonance absorption in the center of the profile is saturated at much lower intensities than the off-resonant wings.[7] Therefore, as intensity rises, absorption in the wings rises faster than absorption in the center, leading to a broadening of the profile. Radiative broadening occurs even at very low light intensities.

The experiment described in this paper is part of the advanced optics laboratory at Miami University, which is offered every year. The laboratory is focused alternately on either "optics and laser physics" or "atomic and molecular spectroscopy."[8] The SAS setup is built by the students in the advanced optics and laser physics laboratory as an assignment. This assignment includes the construction of the frequency-narrowed, tunable external cavity diode lasers.[2,4,9] Sophomore students visit the advanced optics laboratory to see a demonstration of SAS.

II. BASIC SAS SETUP

Figure 1 shows the basic setup for SAS, comprising of three frequency-scanning laser beams (one strong and two weak), propagating through a sample of atomic vapor. In our

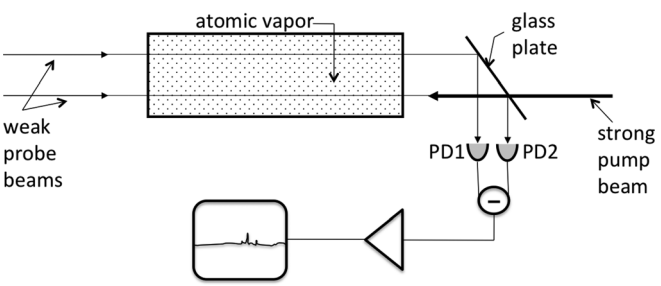

Fig. 1. Basic schematic for SAS. The outputs from photodiodes PD1 and PD2 are subtracted from each other, amplified, and displayed on an oscilloscope.

setup, we used room-temperature Rubidium vapor (72% ^{85}Rb and 28% ^{87}Rb). The goal of SAS is to study the Doppler-free hyperfine structure of Rb with linewidths approaching the natural linewidths. One of the two weak probe beams overlaps with the strong pump beam, which propagates in the opposite direction. The atoms moving perpendicular to these overlapped beams are simultaneously in resonance with both the strong and the weak beams, owing to the absence of any Doppler shifts. Specifically for these atoms, their absorption is saturated by the strong beam, which means that the weak probe passes through without being absorbed. This results in Doppler-free "holes" being "burnt" into the Doppler profile at the site of the hyperfine transitions.[10]

Doppler-broadened absorption peaks are shown in Fig. 2(a) for a weak frequency-scanned laser beam propagating through the Rb vapor. Shown is the output from PD1 when the strong pump beam is not allowed to enter the vapor cell. When the strong pump beam is allowed to enter the vapor cell, Doppler-free "hole-burning" is observed in the absorption profile measured by PD2, as shown in Fig. 2(b). Figure 2(c) shows the intensity difference between PD1 and PD2. This figure shows that the Doppler-free hyperfine spectral features in ^{85}Rb and ^{87}Rb that were previously obscured by Doppler broadening are revealed by SAS. The laser intensity used is less than the saturation intensity which is defined as the intensity at which the probability of a Rb atom being found in the excited state is 1/4. The saturation intensity for ^{85}Rb is 1.64 mW/cm^2.[7] A laser frequency scan across the $F_g = 2 \leftrightarrow F_e = 3, 2, 1$ transitions of ^{87}Rb is shown in Fig. 2(d). Figure 2(e) shows the results of a frequency scan across the $F_g = 3 \leftrightarrow F_e = 4, 3, 2$ transitions of ^{85}Rb. Each of these three hyperfine transitions is individually marked in Figs. 2(d) and 2(e). As is well-known, a characteristic of SAS is that we observe, in addition to the three hyperfine transitions, three "crossover" absorption peaks of similar width, but larger amplitude, located exactly midway between each pair of hyperfine transitions.[10]

The detection and amplification circuits and the optics employed in our setup closely follow the specifications described in an earlier work.[4] Constructing the SAS setup shown in Fig. 1 and obtaining the spectra displayed in Fig. 2 are assignments for the seniors and Masters'-level students in the advanced optics laboratory. The sophomore students who visit the optics laboratory are given handouts of the observed spectra in Fig. 2 and are asked to measure the Doppler linewidths, followed by a linewidth measurement of the SAS hyperfine spectra. The frequency calibration for the

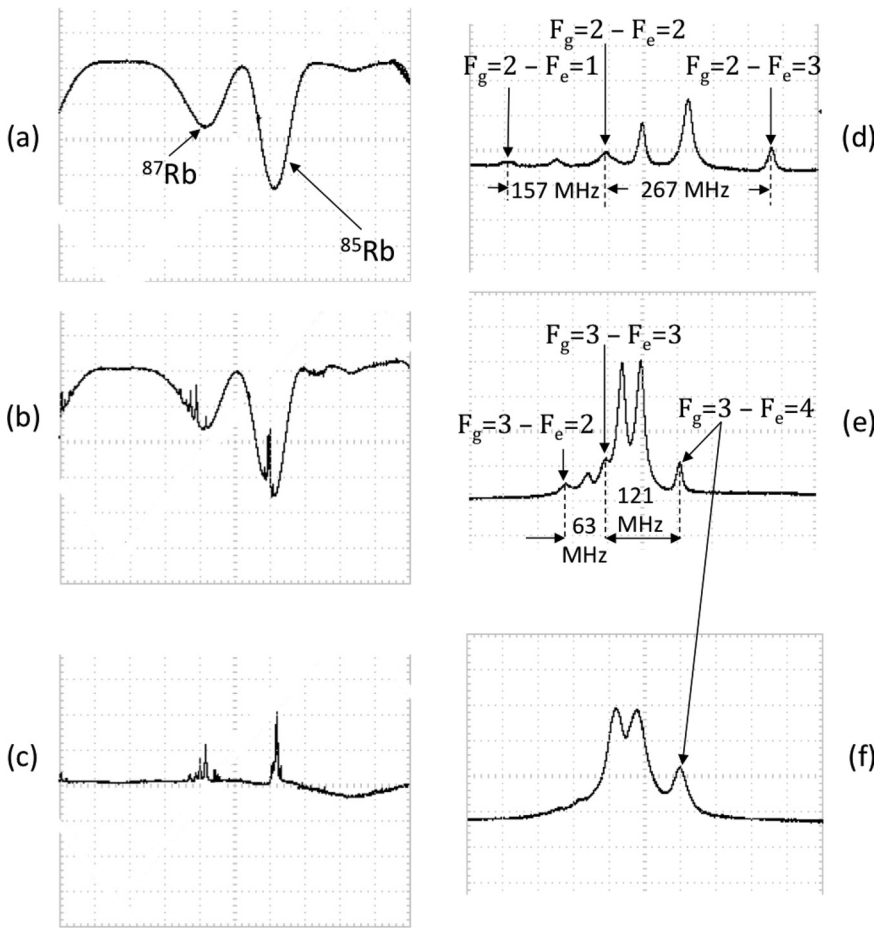

Fig. 2. Snapshots of oscilloscope traces displaying the intensity detected by photodiodes PD1, and PD2 on the y-axes as a function of the "laser frequency" on the x-axes: (a) Doppler broadened absorption spectra for ^{87}Rb (left) and ^{85}Rb (right) detected by PD1 when the strong pump beam is absent. (b) When the strong pump beam is present, "hole-burning" is observed in the absorption spectra detected by PD2. (c) The net absorption spectrum obtained by subtracting the output of PD1 (a) from PD2 (b). Reducing the frequency scan and zooming in on the Doppler-free spectral features in (c) reveals hyperfine spectra for ^{87}Rb and ^{85}Rb, shown in (d) and(e), respectively, for a laser intensity of 6.87 mW/cm^2. The linewidths are measured to be 14.0 MHz, close to the predicted value of 13.6 MHz. (f) Same as (e), except with a higher laser intensity of 46 mW/cm^2. This spectrum shows the power broadening of the ^{85}Rb hyperfine spectrum. The vertical scale is 10× the scale in (e). Note: The horizontal scales for (a)–(c) are 10× those for (d)–(f).

x-axis of the traces shown in Fig. 2 is provided by the known frequency-splittings between the hyperfine lines, as indicated in Figs. 2(d) and 2(e). Using this calibration, the students are asked to go back to Fig. 2(a) and measure the Doppler linewidth. They find that the results are in good agreement with predictions obtained with the theoretical expression[11] for the Doppler linewidth $\gamma_{\text{dopp}} = 2\nu_0\sqrt{2k_BT\ln 2/mc^2}$, where ν_0 is the resonance frequency, which is equal to c/λ_0, m is the atomic mass, and T is the temperature.

III. DEMONSTRATION AND MEASUREMENT OF RADIATIVE BROADENING

The six Doppler-free SAS linewidths in Fig. 2(d) or 2(e) are identical but are not equal to the natural linewidth of 5.98 MHz. The students find that the measured linewidth is a few times larger than the natural linewidth. At this point, the students are introduced to the concept of "power broadening" or "radiative broadening," i.e., line-broadening of the atomic energy levels caused by the presence of the light. This broadening exists even for the rather weak intensities employed in SAS.

The sophomores are given a qualitative demonstration of power broadening by turning up the illumination, well above the saturation intensity The students see how the spectrum shown in Fig. 2(e), taken at an intensity of 7.5 mW/cm^2, transforms into the spectrum shown in Fig. 2(f), taken at an intensity of 50 mW/cm^2. None of the individual hyperfine transitions are discernable in Fig. 2(f), except for the $F_g = 3 \leftrightarrow F_e = 4$ transition in ^{85}Rb.

The students in the advanced optics laboratory, who built the SAS setup, are taught in lecture the well-known theory for radiative broadening[7,11] and are shown the derivation of the power broadened linewidth γ_{rad}

$$\gamma_{\text{rad}} = \gamma\sqrt{1 + I/I_{\text{sat}}}, \tag{1}$$

where γ is the natural linewidth, I is the intensity of the light illuminating the atom, and I_{sat} is the saturation intensity. The students measure the "full width at half maximum" (FWHM) for any one of the six peaks seen in the saturated absorption hyperfine spectrum in either Fig. 2(d) or 2(e) as a function of the laser intensity. For the spectra shown in Figs. 2(d) and 2(e), obtained at an intensity of 6.87 mW/cm^2, the measured linewidths are 14.0 MHz, which is close to the theoretical value of 13.6 MHz, predicted using Eq. (1). It turns out that it is easier to use one of the larger crossover peaks for this measurement. The measured line widths as function of the laser intensity are shown in Fig. 3. The curve in Fig. 3 shows the theoretical prediction made using Eq. (1).

The FWHM measurement can be performed directly with the oscilloscope, provided the following two precautions are taken. First, the oscilloscope input impedance (typically 1 M Ω on most oscilloscopes) must be matched to that of the BNC cable (typically 50 Ω) from the detector-amplifier circuit. We used a 50 Ω inline terminator between the cable and the oscilloscope. This prevents broadening of the spectral features due to an impedance mismatch. Second, at low intensities, the signal strength becomes weak and electronic noise begins to dominate, causing fluctuations in the spectrum. One must avoid the temptation to make measurements on a spectrum that has been averaged over several scans because the average waveform is broadened by the noise,

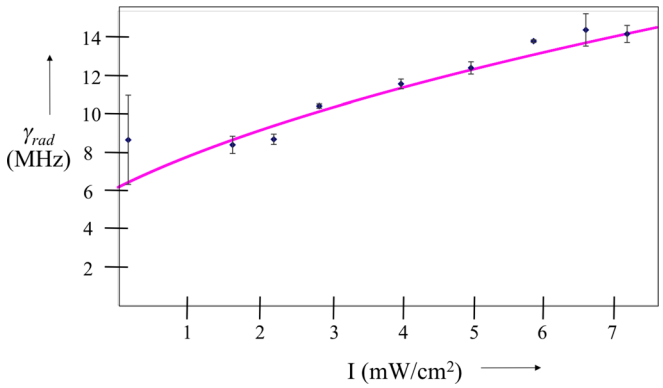

Fig. 3. The radiative broadened linewidth γ_{rad} as a function of intensity. The intensity seen by the atoms is the sum of the strong pump beam and the counter-propagating weak beam. The curve shows the theoretical prediction made using Eq. (1).

even though it may appear cleaner. At each intensity, we found that it is best to make a FWHM measurement using the data obtained in a single scan and repeat this process several times. At the lowest intensities, we found it necessary to average two or three scans in order to be able to make a reliable FWHM measurement. Three FWHM measurements were taken at each intensity. Each data point in Fig. 3 represents the average of these three measurements and the error bar represents their standard deviation divided by $\sqrt{N}$ where $N = 3$ in our case. This approximate and simple method works reasonably well for the range of intensities shown in Fig. 3. At high intensities, the errors are dominated by uncertainties in determining the baseline, while measuring the FWHM for the hyperfine peaks in Fig. 2(e). If time permits, one may choose to model the hyperfine spectrum as the sum of six Lorentzian peaks. This procedure would automatically take into account the effect of slight increases of the baseline of each Lorentzian due to small contributions from neighboring peaks. For the range of intensities shown in Fig. 3, these errors are small and we chose to ignore them in the interest of having the students finish the lab in a timely manner.

IV. CONCLUSION

Radiative broadening of atomic spectral lines is a well-known result which, to the best of our knowledge, has traditionally not been emphasized in the undergraduate laboratory, especially at the low intensities shown in Fig. 3. We have shown that SAS may be used for a quantitative investigation of radiative broadening of atomic hyperfine structure. This experiment naturally caps off the students' journey in light-matter interaction and spectroscopy, from fine structure and D_1–D_2 lines in an alkali vapor, to hyperfine structure and SAS.

ACKNOWLEDGMENTS

The authors gratefully acknowledge financial support from the Petroleum Research Fund. The authors would like to acknowledge help during the initial setup by Courtney Clarke and Harrison Bourne. The authors are indebted to Michael Eldridge for machining support for our laser systems. The authors are also indebted to the Dean of the College of Arts and Science at Miami University for providing generous

seed funding to our advanced optics and lasers teaching laboratory for undergraduates and first-year Masters' students.

[a]Electronic mail: balis@muohio.edu

[1]D. W. Preston and E. R. Dietz, *The Art of Experimental Physics* (Wiley-VCH, Hoboken, New Jersey, 1991), pp. 241–263.
[2]C. E. Wieman and L. Hollberg, "Using diode lasers for atomic physics," Rev. Sci. Instrum. **62**, 1–20 (1991).
[3]For a recent discussion of SAS which includes a brief historical review, see, for example, G. He and S. H. Liu, *The Physics of Nonlinear Optics* (World Scientific Publishing Co., Hackensack, New Jersey, 2003), pp. 377–386.
[4]K. B. MacAdam, A. Steinbach, and C. Wieman, "A narrow-band tunable diode laser system with grating feedback, and a saturated absorption spectrometer for Cs and Rb," Am. J. Phys. **60**, 1098–1111 (1992).
[5]D. W. Preston, "Doppler-free saturated absorption: Laser spectroscopy," Am. J. Phys. **64**, 1432–1436 (1996).
[6]D. Budker, D. J. Orlando, and V. Yashchuk, "Nonlinear laser spectroscopy and magneto-optics," Am. J. Phys. **67**, 584–592 (1999).
[7]See, for example, H. J. Metcalf and P. van der Straten, "Laser Cooling and Trapping," (Springer-Verlag, New York, 1999).
[8]J. Blue, S. B. Bayram, and S. D. Marcum, "Creating, implementing, and sustaining an advanced optical spectroscopy laboratory course," Am. J. Phys. **78**, 503–509 (2010).
[9]A. S. Arnold, J. S. Wilson, and M. G. Boshier, "A simple extended-cavity diode laser," Rev. Sci. Instrum. **69**, 1236–1239 (1998).
[10]D. A. Smith and I. G. Hughes, "The role of hyperfine pumping in multilevel systems exhibiting saturated absorption," Am. J. Phys. **72**, 631–637 (2004).
[11]See, for example, P. W. Milonni and J. H. Eberly, *Laser Physics* (Wiley, New York, 2010).

Tangent Galvanometer

The tangent galvanometer, invented in 1837, is still in use: I recently visited an institution where it was being used to measure the horizontal component of the magnetic field of the earth. This example in the Greenslade Collection was made by J. H. Bunnell of New York. The company, still in existence, was founded in 1878 by Jessie Bunnell, a pioneering Civil War telegraphist, and originally specialized in making telegraph instruments. Later, the company branched out and made test instruments that were used by telegraphers and other electricians of the era. This is a top-of-the-line model, with multiple coils to give a wide range of current sensitivities. (Notes and photograph by Thomas B. Greenslade, Jr., Kenyon College)